Scholars' Mine

2015

Determination of setting times by shear wave velocity evolution in fresh mortar using bender element method

Jianfeng Zhu

Follow this and additional works at: https://scholarsmine.mst.edu/masters_theses

Part of the Civil Engineering Commons, and the Materials Science and Engineering Commons
Department:

Recommended Citation

DETERMINATION OF SETTING TIMES BY SHEAR WAVE VELOCITY

EVOLUTION IN FRESH MORTAR USING BENDER ELEMENT METHOD

by

JIANFENG ZHU

A THESIS

Presented to the Faculty of the Graduate School of the

MISSOURI UNIVERSITY OF SCIENCE AND TECHNOLOGY

In Partial Fulfillment of the Requirements for the Degree

MASTER OF SCIENCE IN CIVIL ENGINEERING

2015

Approved by

Dr. Bate Bate, Advisor
Dr. Kamal H. Khayat, Co-Advisor
Dr. Hefu Pu

ABSTRACT

This study aims at using modified bender element (BE) method to monitor the shear wave velocity (V_s) of mortar at early-age and determine initial and final setting times with the V_s method. Modifications of the traditional BE method have been made to overcome the aggressive cementitious environment and eliminate electromagnetic coupling. BE has been successfully employed in mortar samples with and without admixtures to evaluate the evolution of V_s during the early age (first 24 hrs) of hydration. An energy approach method of determining the first arrival time of S-wave has been proposed. Pulse wave velocity test, penetration resistance test and calorimetry test were carried out to comprehensively evaluate the setting process. The evolutions of Young's modulus E, shear modulus G, bulk modulus K, and Poisson's ratio v with time were then determined based on V_s, V_p and r measurements.

Log-normal distribution and soil-water characteristic curve (SWCC) were used to fit the V_s-time relationship. It was found that the time corresponding to the largest slope (i.e. maximum increasing rate) of the V_s curve corresponds to the final setting time. The initial setting time shows a linear relationship with the first inflection point and parameter a in SWCC equation. This proposed method of determining setting times with V_s had a high accuracy ($R^2=0.98$). With the non-destructive nature and reliable results, bender element method of obtaining V_s and determining set times has a potential application in the cement industry.

ACKNOWLEDGMENTS

I would like to thank all those who helped me during this research. First and foremost, I would like to express my deepest gratitude to my advisor, Dr. Bate Bate. It has been an honor to be his research student. His valuable insights and suggestions have helped me to overcome many hurdles during this work. I am grateful to him for the advice and guidance he gave me throughout my master program.

Further, I thank Dr. Kamal H. Khayat and Dr. Hefu Pu for being part of my thesis committee, for taking the time to read through my thesis and for providing additional helps in satisfying my thesis requirements. Thanks CIES and ACML at Missouri S&T for providing equipment in this research.

Many thanks to my lab mates Xin Kang, Junnan Cao, Song Wang, Kerry Magner, and my dear friend Devin Cornell, for their helps during this work.

Finally, I would like to thank my beloved family for their unconditional love and emotional support in all my pursuits.

TABLE OF CONTENTS

LIST OF ILLUSTRATIONS

LIST OF TABLES

1. INTRODUCTION

The early age properties of cement based materials are significant for the quality and durability of concrete structures. In general, it is very difficult to measure properties at the early age, where kinetic process of hydration reactions occurs (Kjellsen and Detwiler 1992). Non-destructive testing (NDT) is often used to monitor properties changes of cement based materials, which is highly recommended for quality control and quality assurance (Birgul 2009, Yaman et al. 2001, Liang and Wu 2002). Among the available non-destructive tests, ultrasonic pulse velocity (UPV) is widely used because the primary wave (P-wave, or compressive wave) can be detected easily. P-wave is very sensitive to the presence of air voids in paste, mortar, and concrete (Sayers and Dahlin 1993). However, P-wave velocity (V_p) in water is on the same order of magnitude of V_p in a fresh concrete. Therefore, P-wave is not sensitive to the property changes during curing process. On the other hand, shear wave (S-wave) is not sensitive to the presence of water, but to the solid skeleton of a material. Therefore, S-wave is promising in monitoring of the initial state of a curing cementitious material. In this study, shear wave is proposed to monitor the setting process of cementitious materials.

There are very limited tools available for measuring the S-wave in concrete (Soliman et al. 2015). Bender element (BE) is a sensor made by piezoceramics, which are commonly used to evaluate the shear wave velocity of a soil (Dyvik and Madshus 1985; Viggiani and Atkinson 1995; Lee and Santamarina 2005; Bate et al. 2013; Kang et al. 2014). Application of BE in cementitious materials is very limited (Zhu et al. 2011, Liu et al. 2014). Modifications to the traditional BE is needed for aggressive cementitious

environment. This study proposed using BE to monitor the shear wave velocity of freshly casted mortars, and determine their initial and final setting times.

The objective of this study is to evaluate the evolution of V_s in the early age of mortars by using modified bender elements, to develop a method of determining setting times with V_s, and to have a better understand of the mortar behavior at early age. To achieve this objective, the following steps were taken in this study. (1) Modifications of traditional BE have been made to overcome the aggressive cementitious environment, eliminate electromagnetic coupling, avoid interference of P-wave, balance the wavelength ratio (R_d) and damping ratio etc. (2) BE has been successfully employed in mortar samples with and without admixtures, to evaluate the evolution of V_s during the early age (first 24 hrs) of hydration. (3) A new method of determining the first arrival time of S-wave has been developed. (4) Pulse wave velocity test, penetration resistance test and calorimetry test have been used to comprehensively evaluate the setting process, therefore, the evolutions of Young's modulus E, shear modulus G, bulk modulus K, and Poisson's ratio v with time were obtained based on V_s, V_p and r. (5) A method of determining setting times with V_s has been proposed.

2. LITERATURE REVIEW

2.1. IMPORTANCE OF SET TIMES

The properties of hardened cement based materials (pastes, mortar, and concrete) have been well studied in traditional research, but the early age (first 24 hours) properties are fairly unknown. This is partially because of the complicated cement hydration reactions and the huge variation of properties (Ma 2013). Two key parameters to characterize an early age cementitious material are initial and final setting times. Initial setting time indicates the time when cementitious materials are sufficiently rigid to withstand a certain amount of pressure, at which materials start losing its plasticity. Final setting time indicates the time when the development of strength and stiffness starts, as well as its plasticity is completely lost. Set times are important for transportation, placing, compaction, and removal of formwork (Garnier et al. 1995; Li et al. 2007).

2.2. METHODS OF SET TIMES DETERMINATION

There are some laboratory methods to measure setting times of cement based materials, such as (1) Mechanical method: Vicat needle test (ASTM C 191) for paste and penetration resistant test (ASTM C 403) for mortar and concrete. (2) Isothermal calorimetry method (Zhang et al. 2015, Ge et al. 2009, Rahhal and Talero 2009, Sandberg and Liberman 2007, Hofmann et al. 2006). Besides above laboratory methods, a field test method is needed to monitor the curing process for quality assurance and quality control (QA/QC). The following methods can be used in the field. (1) Ultrasonic pulse velocity measurement (Trtnik et al. 2008, Chung et al. 2012). (2) Hydraulic pressure variations (Sofiane Amziane 2006). V_P is not sensitive to early age stiffness evolution due to the

high V_p value of water. Hydraulic pressure requires tall and large specimen and accurate

pressure sensors. Therefore, both methods are not convenient for field application.

Soliman et al. (2015) and Zhu et al. (2011) used shear wave velocity to determine setting

time. However, there are some limitations in those methods; they are either too bulky or

less length of measuring time. Due to the fact that V_s is sensitive to the skeleton contacts

of a material, it holds the promise of being used in the field as an NDT monitoring tool.

2.3. CHALLENGES FOR USING BENDER ELEMENT

The use of shear wave in cement based material is very rare, and it is difficult to

detect the arrival of shear wave because: (1) It usually comes after primary wave, which

introduces a problem of separating or differentiating S-and P-wave. (2) Reflected,

refracted or scatted waves have a high possibility to hinder the arrival of S-wave (Landis

and Shah 1995). It is important to note that Birgul (2009) developed a method named

Hilbert transformation of waveforms to determine S- and P-wave velocity in hardened

concrete, modulus of elasticity and Poisson's ratio were calculated based on V_s and V_p

together with the density of concrete. But just like most of the NDT research, the

application of these measuring methods is limited in the hardened state of materials.

Therefore, the development of V_s in all age, especially the early age, of cementitious

materials is necessary.

Due to its small size, low cost, simplicity to make and non-destructive nature,

bender element is wildly used for measuring the small-strain shear modulus G_{max} of a soil

(Dyvik and Madshus 1985; Viggiani and Atkinson 1995; Lee and Santamarina 2005;

Bate et al. 2013; Kang et al. 2014), which often has smaller stiffness than a hardened

cementitous material. However, its application in cementitous materials, such as cement

paste, mortar and concrete is very limited, because of the aggressive environment introduced by cement hydration, high damping ratio, fast evolution of stiffness and strength. Zhu et al. (2011) tried to adapt BE in fresh cement paste, but the received signals still mixed with P-wave, and the measuring time was very limited (0-6 h).

6

3. MATERIALS AND MIXING DESIGN

3.1. MATERIALS

Ordinary Type I Portland cement (QUIKRETE, Atlanta, GA) was used in all

tests, in compliance with ASTM C 150 and Federal Specifications for Portland cement.

The chemical composition of Portland cement is listed in Table 3.1 (Mehta and Monteiro,

2006). Poorly-graded Missouri River sand (portion passing through No. 4 sieve) with D_{50}

of 0.7 mm and C_u of 2.74 was used in this study. Grain size distribution curve was shown

in Figure 3.1. Two chemical admixtures were used to introduce variation of setting time.

Hydration controlling admixture (MasterSet Delvo, Cleveland, Ohio) retarded setting

time by controlling the hydration of Portland cement. Non-chloride accelerating

admixture (MasterSet AC 534, Cleveland, Ohio) was used to accelerate setting time.
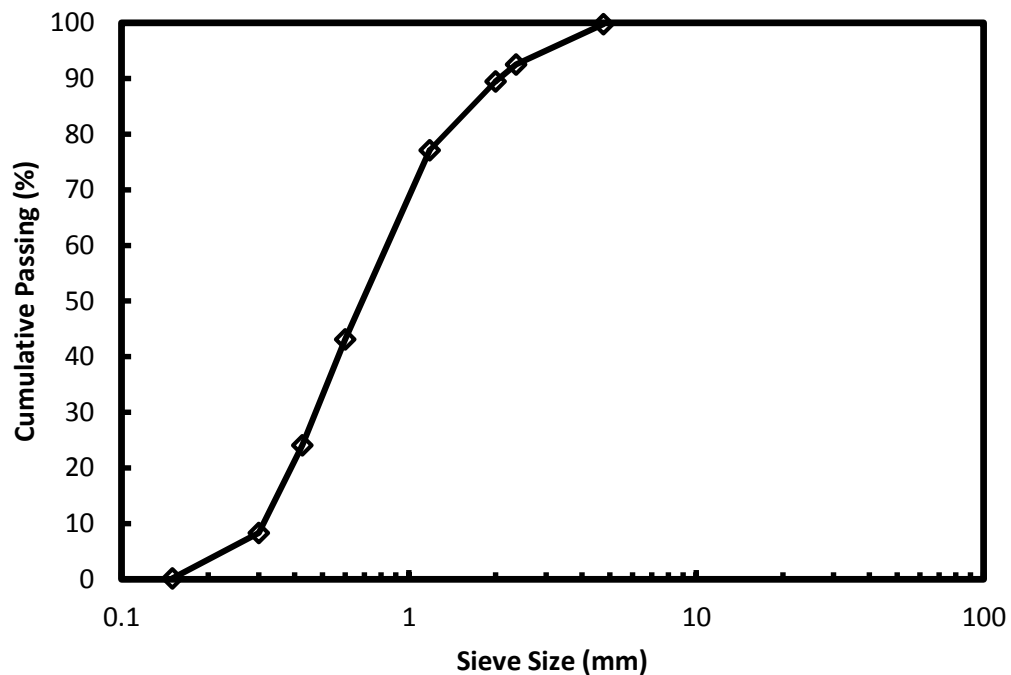
Figure 3.1. Grain-Size Distribution of Sand

Table 3.1. Chemical Composition of Portland Cement (Mehta and Monteiro, 2006)

Chemical component	%
CaO	65.0
SiO_2	21.1
Al_2O_3	6.2
Fe_2O_3	2.9
SO_3	2.0
Rest	2.8

3.2. MIXING DESIGN

There were six mortar mixtures used in this investigation (Table 3.2). Mortar

mixtures were designed with water cement ratio (w/c) of 0.50, 0.43, and 0.37, which were

subsequently named Mix 1, Mix 2, and Mix 3, respectively. Mix 1 was performed three

times to determine the repeatability of bender element test. The accelerator and retarders

were selected based on the criteria given in ASTM C 494: The allowance for normal

variation of initial setting time is (1) between 1 hour and 3.5 hours later when using

retarder, and (2) between 1 hour and 3.5 hours earlier when using accelerator. Mix 4 and

Mix 6 (modified from Mix 2) contained 3 fl oz/cwt (195 ml/100kg) and 3.4 fl oz/cwt

(220 ml/100kg) hydration controlling admixtures (retarders), respectively. Mix 5

contained 23 fl oz/cwt (1500 ml/100kg) accelerating admixture. The mixing procedure of

the mortar mixtures is in compliance with ASTM C 305, Section 8.

Table 3.2. Mixture Design of Mortars

Mix design	Mix 1*	Mix 2	Mix 3	Mix 4	Mix 5	Mix 6
w/c	0.50	0.43	0.37	0.43	0.43	0.43
Cement (kg/m^3)	673	713	751	713	713	713
Sand (kg/m^3)	1137	1203	1267	1203	1203	1203
Water (kg/m^3)	337	313	277	313	313	313
Unit weight (kN/m^3)	21.34	22.28	22.63	22.08	21.78	22.08
Retarder (ml/100kg)	--	--	--	195	--	220
Accelerator (ml/100kg)	--	--	--	--	1500	--

* repeated three times to determine the relative error

4. EXPERIMENTAL PROGRAM

Bender element test, penetration resistance test, ultrasonic pulse wave test, and calorimetry test were performed with six mortar mixtures (Table 4.1).

Table 4.1. Experimental Matrix

	Mix-1	Mix-2	Mix-3	Mix-4	Mix-5	Mix-6
BE test	√	√	√	√	√	√
Penetration test	√	√	√	√	√	√
UPV test	√	√	√	√	√	√
Calorimetry test	√	√	√	√	√	√

4.1. DESIGN OF THE BENDER ELEMENT SYSTEM

A bender element testing system for cementitious materials, consisting of a signal generation and acquisition system, a wooden formwork, and three pairs of bender elements, is designed in this study. Figure 4.1 illustrates details of setup.

4.1.1. Bender Element. There were a few design concerns upon the fabrication of bender elements. (1) Cementitious materials are corrosive with high pH and the products of their hydration reactions, which are hostile to the coating layers of a traditional bender element. (2) In addition, the stiffness and the damping ratio (energy dissipation) of cement paste, mortars and concretes during initial curing period (up to 72 hours) evolve rapidly as those cementitious materials change from slurry state to a semi-solid state. As a result, the resonant frequency of these materials will increase drastically (estimated to be from 100 Hz to 14,000 Hz), while the attenuation of the received electrical signals will likely decrease. (3) Above changes will also influence the geometry of the concrete

specimen to accommodate the requirement for travel distance to wavelength ratio (R_d ratio), which should be no less than two to avoid the near-field effect (Marjanovic and Germaine, 2013). Due to the above stated concerns, modifications to the fabrication process of bender element, the signal emitting and receiving procedures as well as the geometry of the testing specimen are warranted.
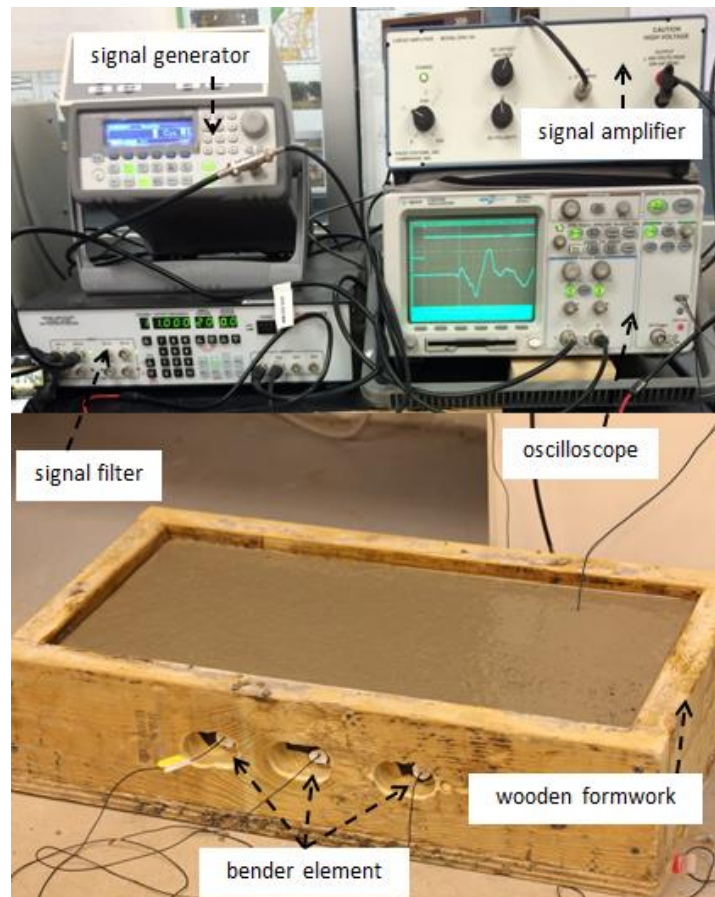

Figure 4.1. Bender Element Testing System for Cementitious Materials

The well-documented traditional fabrication procedures of bender element, including connection of coaxial cable, soldering, circuit checking, polyurethane coating, silver conductive coating, and epoxy coating (Bate et al. 2013; Kang et al. 2014; Lee and

Santamarina 2005) were modified to accommodate tests in cement-based materials. Two-layered brass-reinforced piezo actuators (T226-H4-503Y, Piezo Systems, Inc., Woburn, MA) were cut into bender element plates with dimension of $23 \times 11.5 \times 2$ mm (length $\times$ width $\times$ thickness). This size is larger than the typical sizes (ranging from $12 \times 5 \times 0.5$ mm to $20 \times 12.7 \times 2$ mm) (Yamashita et al. 2009) in soil testing with the consideration of the long travel distance in a large specimen and of the initially paste-type materials. Parallel-type connection was adopted over series-type connection for strong received signals (Lee and Santamarina 2005).

Tradition coatings on a BE are polyurethane, silver paint, epoxy. Polyurethane was still used. Three to five layers of polyurethane coating were applied to ensure good contacts between polyurethane and the piezoceramics plates and good waterproof ability. However, the following modifications were made.

(a)   Silver conductivity coating on bender element provides electrical shield to prevent cross-talking (Lee and Santamarina 2005). However, it was not used in the study because (1) no obvious improvement in the quality of signals was observed using silver painting in a side-by-side comparison test on dry sands using bender elements with and without silver conductivity coating, and (2) bender elements are more prone to electrical short-circuiting during silver coating procedure, which leads to lower rate of successful fabrication of bender element, and (3) sufficient electrical shield could be provided by parallel bender element made with twisted coaxial cable with grounding (drain wire embedded into the testing material) (Montoya et al. 2012).

(b)   PVC cement was used in this study instead of the often-used epoxy due to its higher moisture resistance, good flexibility, good chemical resistance, and good

durability during multiple tests. In order for better mechanical bond of PVC cement, a layer of Oatey purple primer was recommend by Montoya et al. 2012 to roughen up the surface of the polyurethane-coated piezoceramic plate, as shown in Figure 4.2.

(c)   Bender element was wrapped by a layer of plastic bag after all the coatings were done.
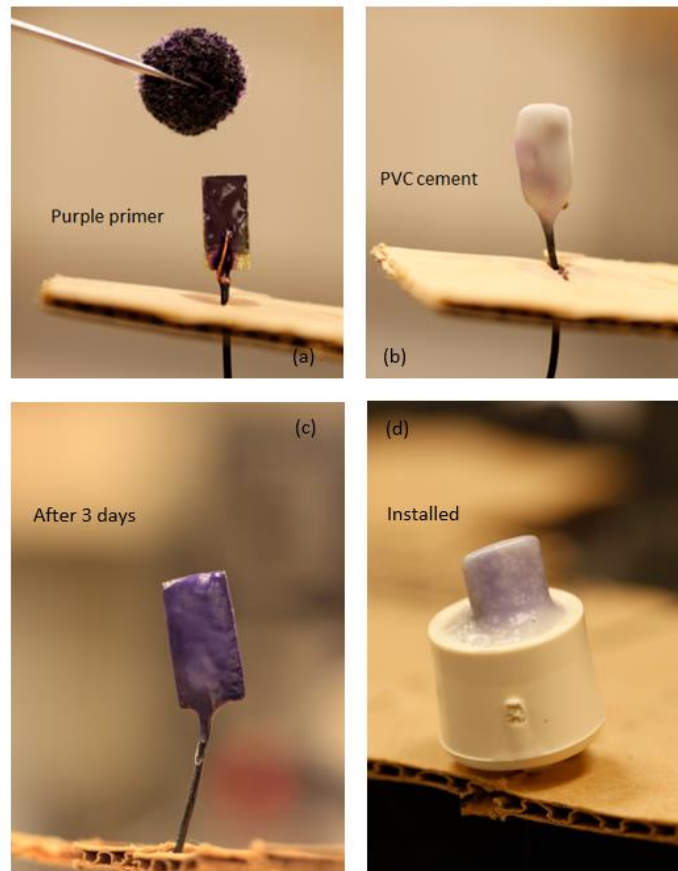

Figure 4.2. PVC Cement Coating: (a) Roughing Up the Surface of the Transducer with Purple Primer; (b) Coating with PVC Cement; (c) Bender Element Three Days after PVC Cement Coating; (d) Bender Element after Installed in a Socket

As a result, the coatings on a BE in this study were in the order of polyurethane, purple primer, PVC cement, and plastic wrap (Figure 4.3).
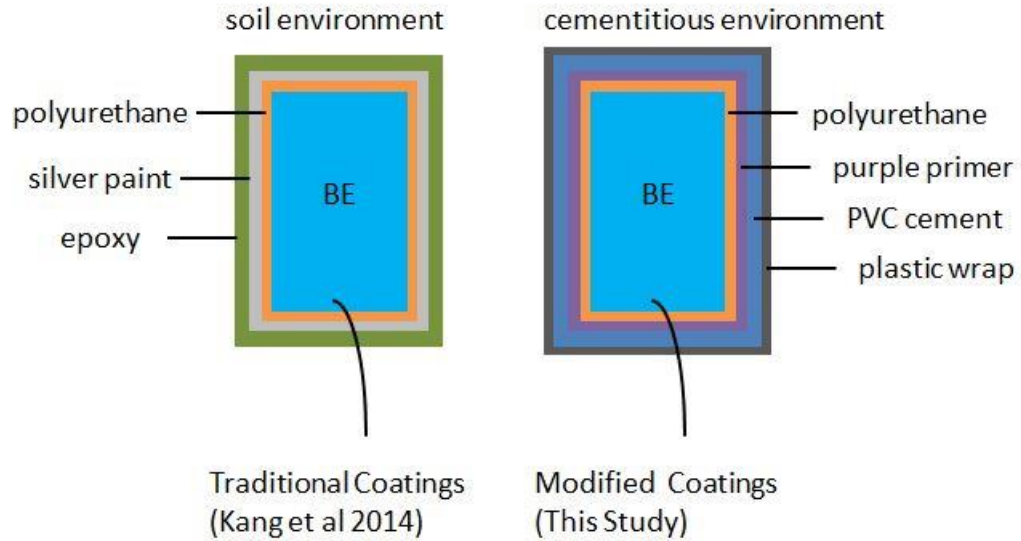
Figure 4.3. Coatings of Bender Element

4.1.2. Wooden Formwork. The dimensions of the wooden formwork (Figure 4.4) were 61.0 cm (24 inch) in length, 30.5 cm (12 inch) in width, and 14.0 cm (5.5 inch) in height (Figure 4.3). The distance between bender element and the surface of mortar was 3.8 cm (1.5 inch); and the volume of mortar was 21.26 dm^3 (0.75 ft^3). The tip-to-tip distance (travel distance of S-wave) of bender elements was 27.0 cm (10.6 inch). The width of the formwork (30.5 cm) was selected by considering the following aspects. (1) There is inherent system lag in the bender element coatings and the electrical system (Montoya et al. 2012), approximately (20 +/- 10 μs) from more than three repeated tip-to-tip measurements on four pairs of BE units. Besides, the stiffness of hardened cementitious materials is higher than that of common soils. Therefore, longer travel distance is required so that the travel time is big enough to offset the time lag. (2) On the other hand, the travel distance should not be too long to significantly dampen the received signals. As a trade-off, travel distance was chosen to be 27.0 cm, so that the

travel time was at least > 8 times the travel distance while maintaining high quality
received signals.
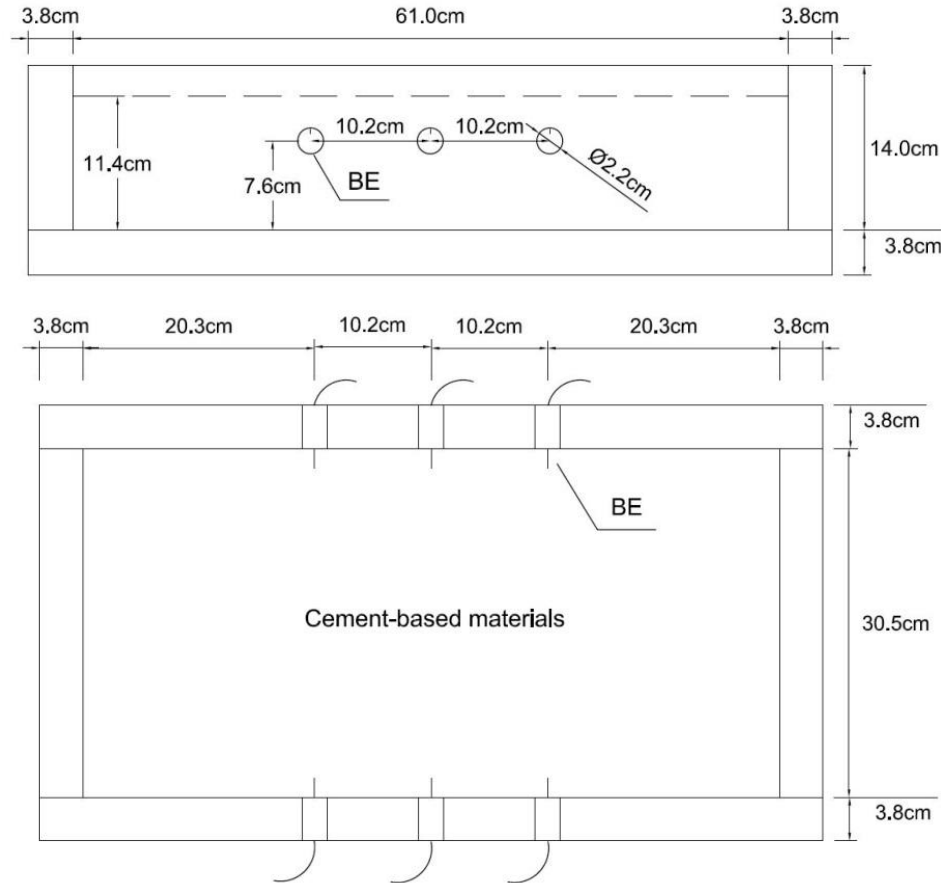
Figure 4.4. Schematic Setup of the Wooden Formwork and Arrangement of Bender
Elements
Top: Side View, Bottom: Top View

The 3.8 cm thick wooden formwork was rigid enough to resist any lateral
movement due to the lateral pressure exerted by mortar and to ensure the tight contact
between bender element and the mortar. The formwork can be reused easily by removing
the concrete specimen through the screw connections and the lubricating oil applied to
the inner surfaces. Three pairs of bender elements were installed in the pre-drilled holes

with diameter of 2.2 cm (0.88 in), aligning perpendicularly to the bottom of the formwork so that no void would be introduced immediately underneath the benders during placing the mortar mass.

4.1.3. Signal Generation and Acquisition System. The signal generation and acquisition system consists of a 1 mHz -10 MHz function/arbitrary waveform generator (33210A, Agilent, location), a linear amplifier (EPA-104, Piezo Systems), a 4 pole LP/HP filter (3364, Krohn-Hite), and a 100 MHz oscilloscope (54622A, Agilent). The transmitter bender element was excited by both square and sine waves. The excitation frequency was 20 Hz for square wave and ranged from 100 Hz to 14 kHz for sine wave. The amplitude of the waveform generator was 10 V.

To obtain both strong response and weak noise in the received signals, the exciting frequency of the input sine wave was adjusted from 100 to 14, 000 Hz during the curing process of the mortar as its natural frequency change significantly over time. Square wave, containing a wide frequency range which can cover the evolving natural frequency of the mortar, has a fixed input frequency of 20 Hz (Lee and Santamarina 2005; Montoya et al. 2012). The transmitter bender was connected to the amplifier and the receiver bender was connected to the filter. Frequency cutoff was adjusted 1 Hz of high pass (HP) and 50 kHz of low pass (LP) by the filter.

4.2. PENETRATION RESISTANCE TEST

The penetration resistance test was performed with loading apparatus (Acme Penetrometer H-4133, Humboldt Mfg. Co., Elgin, IL) and penetration needles (H-4137, Humboldt Mfg. Co., Elgin, IL) to determine the initial and final setting time of mortar according to ASTM C 403 and AASHTO T197.

The apparatus consists of containers for mortar specimens, penetration needles (H-4137, Humboldt Mfg. Co., Elgin, IL), loading apparatus (Acme Penetrometer H-4133, Humboldt Mfg. Co., Elgin, IL) (Figure 4.5) and tamping rod. Gradually applied a vertical force downward on the specimen until a depth of 1 in (25mm) was reached by needle. The time taken to penetrate 1 in depth was about 10 ±2 s. Six to nine undisturbed readings of penetration resistance were recorded for each test. The bearing areas of the penetration needles were 1, ½, ¼, 1/10, 1/20, and 1/40 in^2 (645, 323, 161, 65, 32, and 16 mm^2). The penetration resistance was calculated by dividing the recorded force by the needle bearing area. Elapsed time was from the time when water was added to cement. For each plot, the initial and final setting time correspond to penetration resistance of 500 psi and 4000 psi (3.5 MPa and 27.6 MPa) respectively.

Figure 4.5. Apparatus of Penetration Resistance Test

4.3. CALORIMETRY TEST

The calorimetry test was carried out to evaluate the heat flow generated by the hydration reaction of cement over time, usually 48 to 96 hours, in compliance with ASTM C 1679. The apparatus (Figure 4.6) consists of I-Cal 8000 Isothermal Calorimeter

(Calmetrix, Inc., Boston, MA) and Calmetrix's CalCommander software, which is
available in CIES at Missouri S&T. A small batch of sample (50g to 150g) from mortar
was placed in a clean reusable plastic cup. Cup was properly sealed to avoid erroneous
measurement data. The lid was immediately closed when performing a test to minimize
heat exchange caused by keeping the lid open. Have the data (mix compositions, total
mass, logging, and mix time) all recorded before placing samples.

Arrhenius' law (Equations 1) describes the temperature dependency of the
hydration rate of cement that the warmer the mortar, the faster hydration is:

$$k = Ze^{-E_a RT} \tag{1}$$

where k is the rate constant for the reaction, Z is a proportionality constant that
various from one reaction to another, E_a is the activation energy for the reaction, R is the
idea gas constant in joules per mole Kelvin, and T is the temperature in Kelvin. (ICal
8000 User Manual) Constant temperature (20.0 °C) was used for all the calorimetry tests.

Figure 4.6. Apparatus of Calorimetry Test (Left: I-Cal 8000 with Computer; Right: I-Cal
8000 Interior)

4.4. UNTRASONIC PULSE VELOCITY TEST

Ultrasonic pulse wave (UPV) test was used to measure the primary wave (P-
wave) velocity evolution in the cement-based materials at early age, in compliance with

ASTM C 597. Ultrasonic Pulse Velocity – Pundit Lab (Proceq Int., Aliquippa, PA)

(Figure 4.7) was applied in this study. Two holes (2 inches in diameter) in the wall of the

mortar

container (8 inches diameter QUIK-TUBE Building Form, QUIKRETE, Atlanta, GA)

were drilled for placing the transducers (Standard 54 kHz Transducer, Proceq Int.,

Aliquippa, PA). An appropriate coupling agent (Vaseline) was applied to either or both

the transducer faces and the specimen surface, in order for a good contact between

transducer and specimen. The face of the transducer was firmly pressed against mortar

surfaces until a stable transit time is displayed on the device. The resolution of transit

time is 0.1 μs. The P-wave velocity was obtained by dividing the travel distance by

transit time. Elapsed time started from the moment when water was added to the cement.
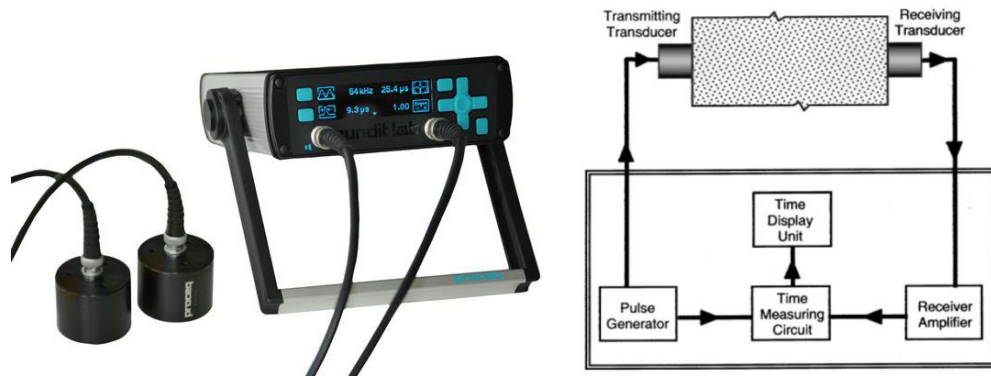
Figure 4.7. Apparatus of UPV Test (Left: Apparatus of UPV Test; Right: Schematic
Setup of UPV Test)

5. RESULTS AND DISCUSSION

5.1. DETERMINATION OF SET TIMES WITH STANDARD PENETRATION METHOD

Penetration resistance of 500 psi and 4000 psi corresponded to the initial and final setting times, respectively. Penetration resistance was plotted against the elapsed time as shown in Figure 5.1. The measured initial setting time ranged from 197 min to 575 min and final setting time ranged from 263 min to 690 min (Table 5.1).

Figure 5.1. Variations of Penetration Resistance with Time

5.2. BENDER ELEMENT TEST RESULT

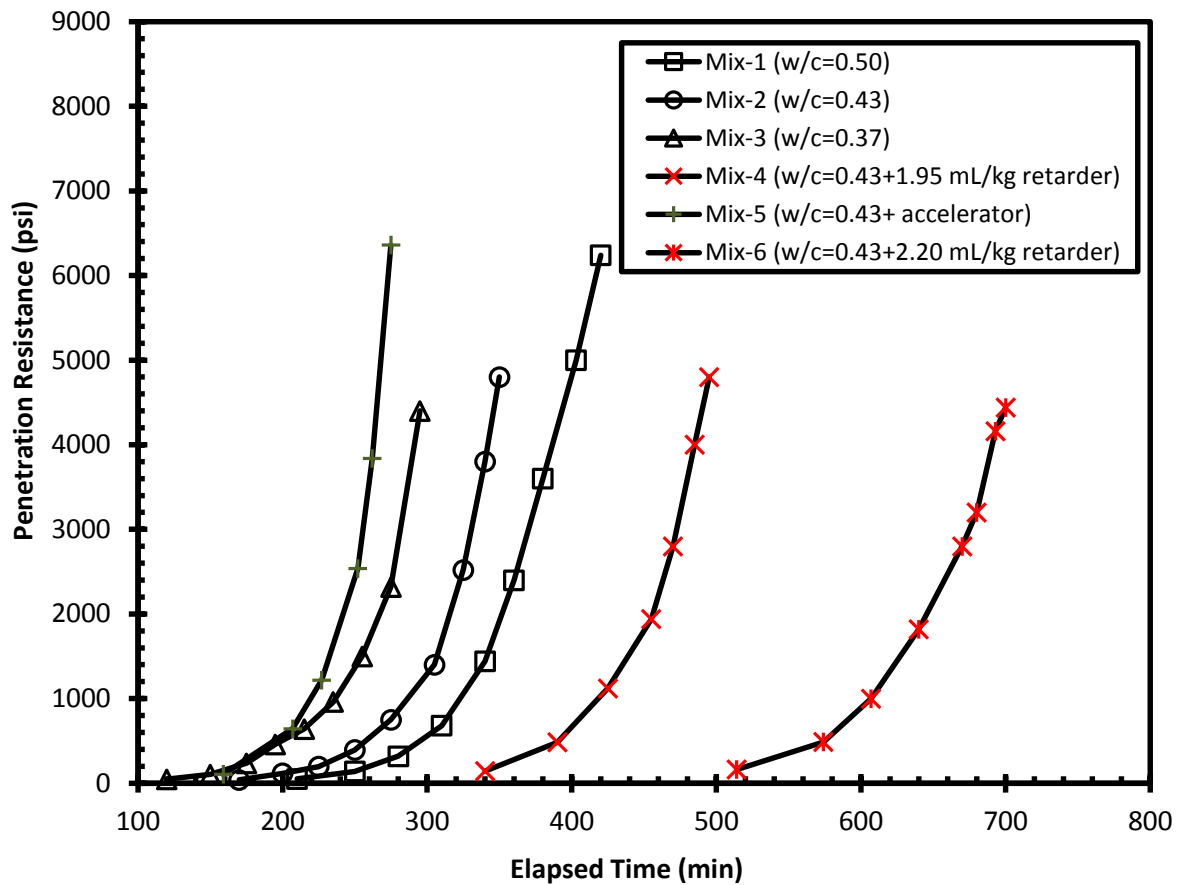**5.2.1. Interpretation of First Arrival Time by Energy Approach.** The

traditional interpretations of first arrival time include peak-to-peak, start-to-start, and half

peak interpretations (Lee and Santamarina 2005; Arulnathan et al. 1998; Leong et al.

2005); however, there is no standard for determining the first arrival time. Equation 2

shows that energy (E) transported by a shear wave is proportional to the square of the

wave amplitude (A). That's because according to Ohm's Law (Equation 3), power (P) is

proportional to the square of voltage (U) while resistor (R) is a constant. Both wave

amplitude and voltage are in the same unit of mV.

$$E \propto A^2 \tag{2}$$

$$P = U^2 / R \tag{3}$$

Energy approach was achieved by taking square value of voltage; as a result, each

point in signals was either zero or positive. The output of square shear wave signal with

mortar mix-1 at 8 hours after water was added to cement, was shown in Figure 5.2, from

which points a, b, c, and d are possible to be manually picked as first arrival time with

traditional methods (Figure 5.2 a), however, it is obvious that point e is the only option

for first arrival time with energy approach (Figure 5.2 b). The benefits of using energy

approach include (1) Easier to identify the first arrival time. (2) Less variability, because

a consistent reading of first arrival time can also be achieved when waveforms are

irregular.

5.2.2. Typical Received Shear Wave Signals. Typical received shear wave

signals shown arrival times vary a lot, ranging from 17 *ms* at 1 h to 186 *μs* at 86 h of

cement hydration for the mortar sample with w/c of 0.50 (Figure 5.3). It was observed that (1) the first arrival time decreased at a rapid rate before initial set (< 5 h) and at a slow rate after 10 h of hydration reaction, and (2) Multi scale of shear wave figures have to be used in order to read first arrival times clearly.
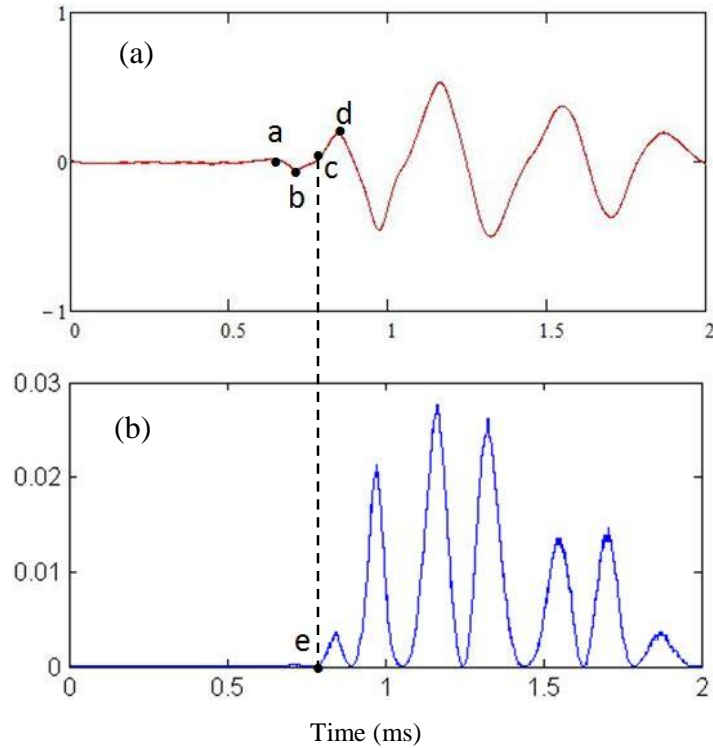
Figure 5.2. Determination of First Arrival Time (a) Traditional Interpretation; (b) Energy Approach

Table 5.1. Initial and Final Setting Times Determined by Penetration Resistance Test

Mortar mixture	w/c	t_i (min)	t_f (min)
Mix-1	0.50	300	385
Mix-2	0.43	260	340
Mix-3	0.37	197	290
Mix-4	0.43+less retarder	392	485
Mix-5	0.43+accelerator	197	263
Mix-6	0.43+more retarder	575	690

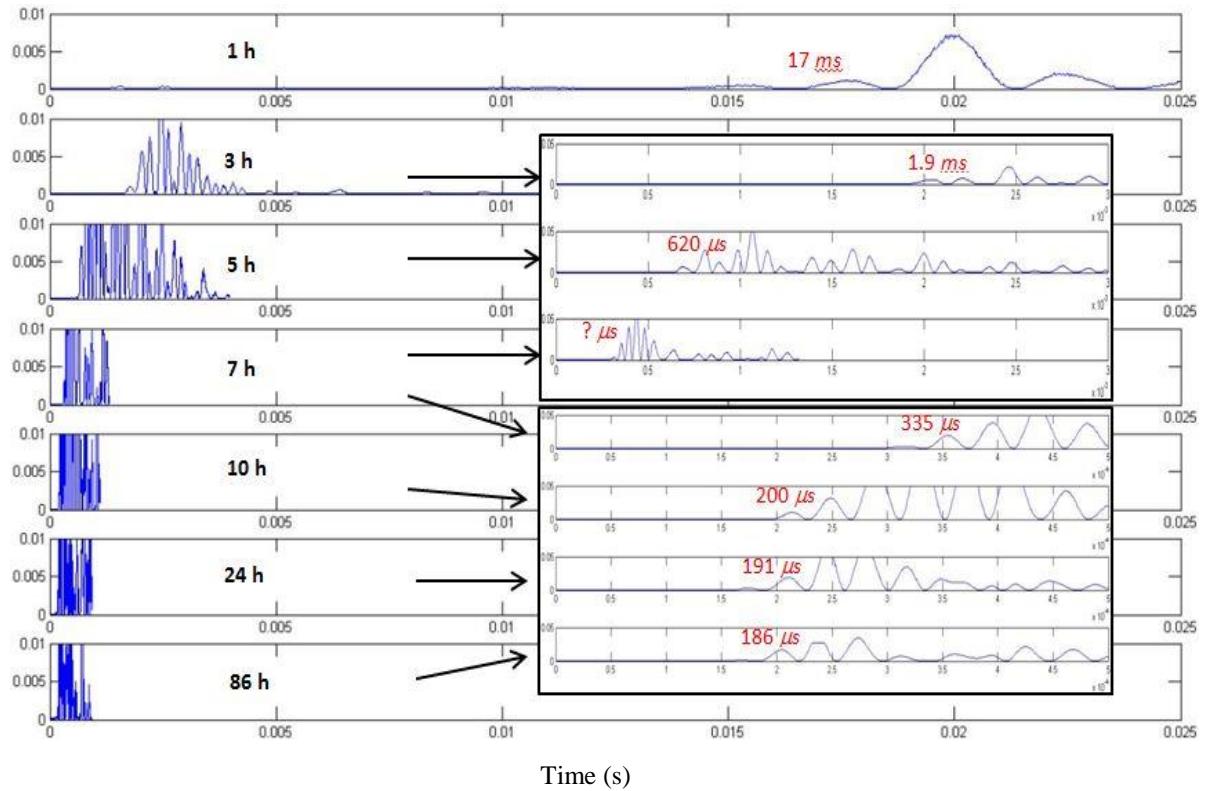Figure 5.3. Typical Received Shear Wave Signals with Different Scales (Mortar Mix-1 with 0.50 of w/c, Sine Waveforms)

In order to achieve clear received signals for the determination of first arrival time (Jovicic et al. 1996), the frequency of input sine signals was needed to adjust to or closed to the highly variable natural frequency of the BE-mortar system. It was noted that excitation frequency did not affect the first arrival time only when clear signals were received at exciation frequencies (4k - 32 kHz) are close to the system natural frequency (approximately 8 kHz) (Figure 5.4). Readings were not possible when excitation frequency was too small (1 kHz) or too large (64 kHz).

5.2.3. Repeatability Analysis of V_s Results. Shear wave velocity results of three pairs of bender elements for Mix-1 using both sine and square incidental waves were shown in Figure 5.5. The maximum standard deviation of V_s at a single time spot is 11.2%. It was also observed that the standard deviation of V_s after 9 h was relatively

large (> 7%). This is because the wave travel time has decreased to a small value (less

than 300 μs), while the inherent system lag remained at a relatively fixed value (20 +/- 10
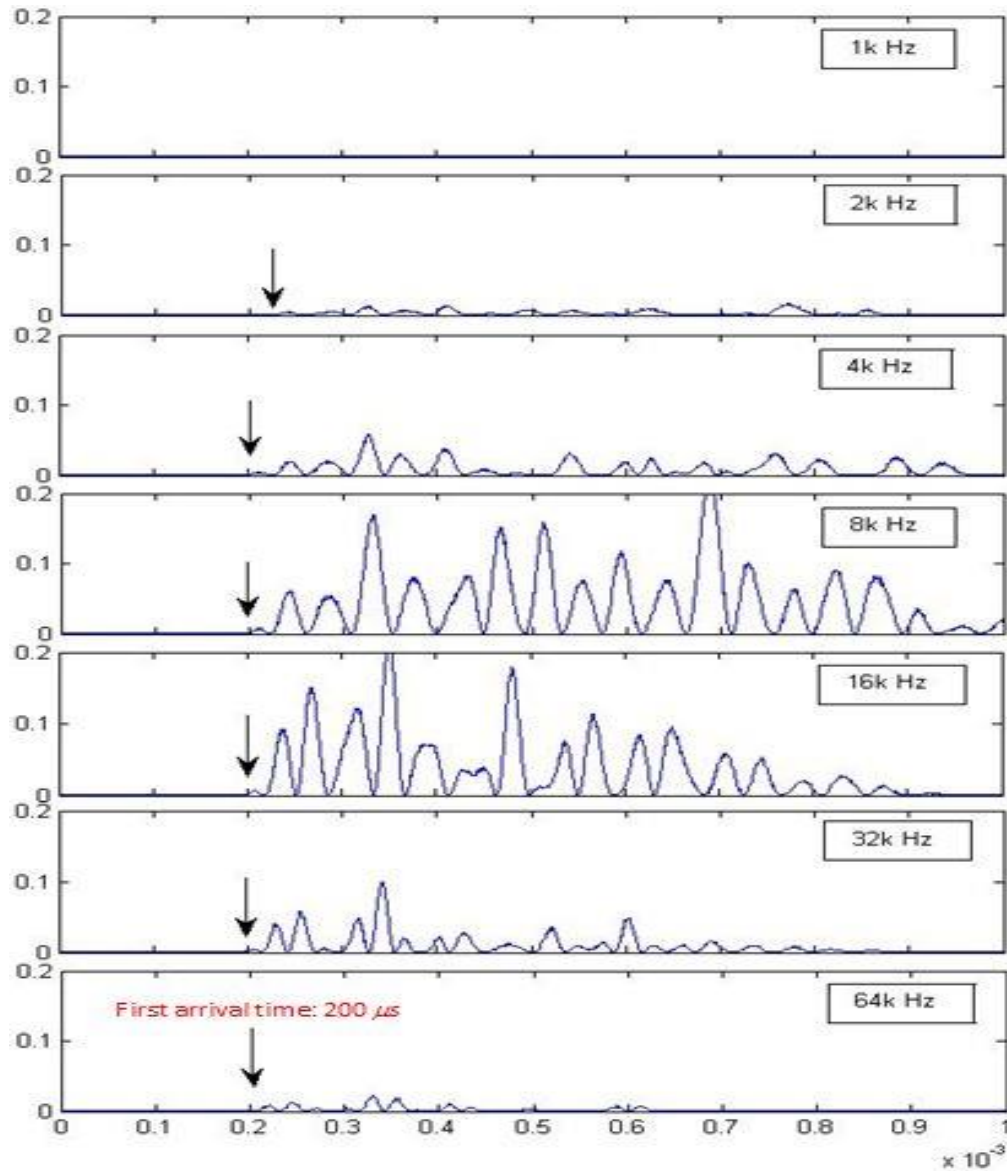
μs).

Figure 5.4. Effect of Frequency Change and Resonant Frequency (Mortar Mix-3 with
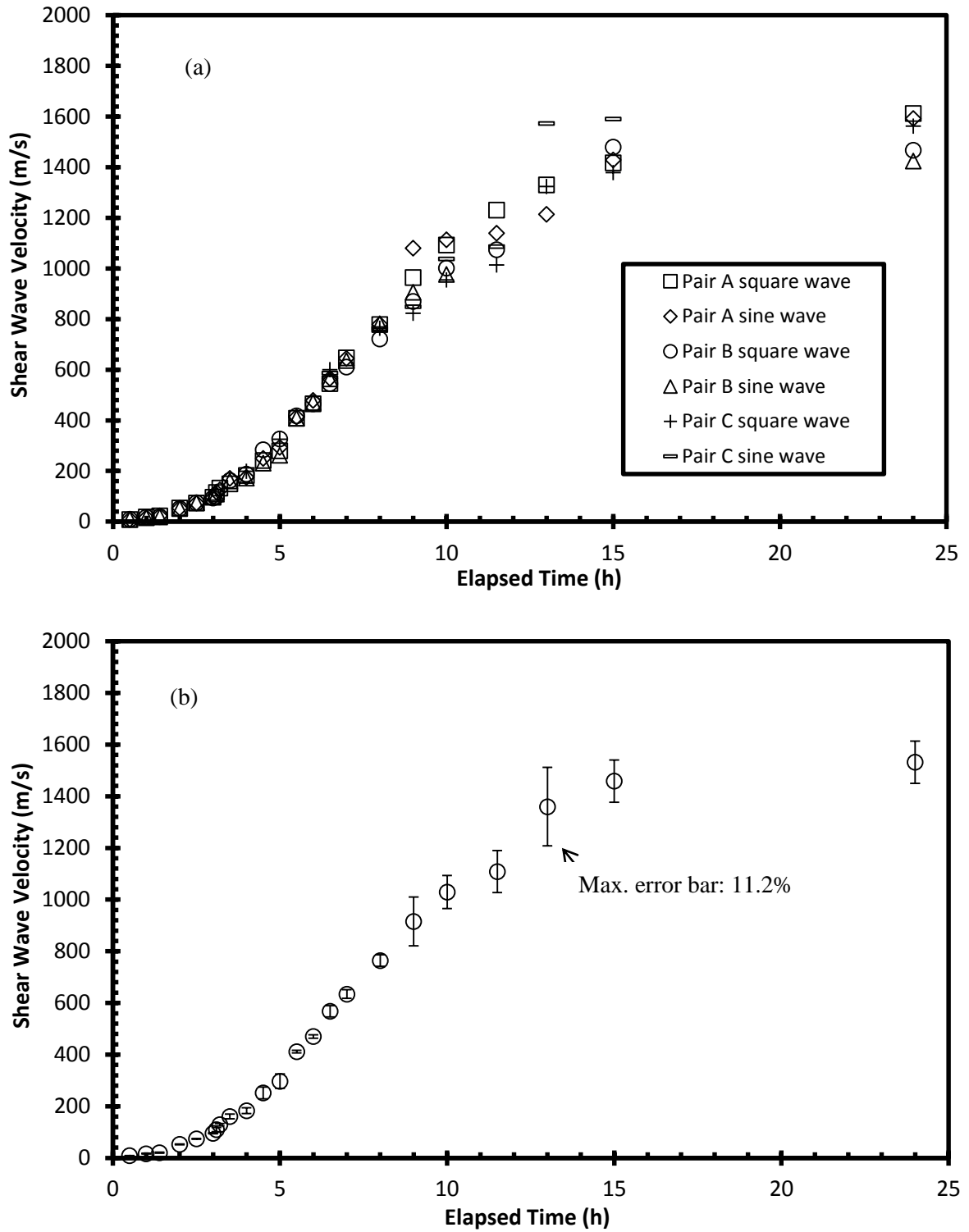0.37 of w/c, Sine Waveforms, at 10 Hours of Cement Hydration)

Figure 5.5. Typical Standard Deviation Analysis of Three Pairs BE with Square/Sine
Waves (a) Six Parallel Signals (b) Standard Deviation

Results of three repeat shear wave velocity tests with w/c = 0.50 mortar are shown in Figure 5.6. Small variation was observed, which indicates that relative reliable V_s results can be achieved with BE for cementitious materials.
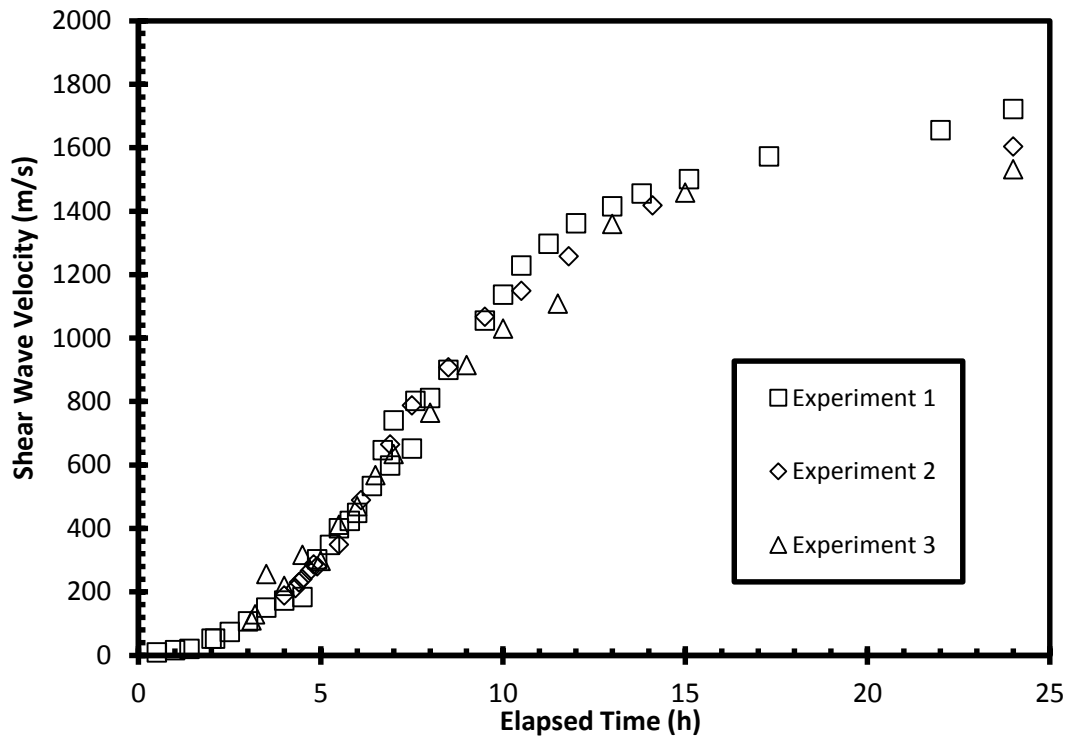

Figure 5.6. Shear Wave Velocity versus Time Curves From Bender Element Tests for Three Repeat Mortar Specimens Using Mix-1 Design

5.3. SHEAR WAVE VELOCITY RESULTS OF MORTARS

Shear wave velocity versus elapsed time relationship of six mortar mixtures are shown in Figure 5.7. The results show that: 1) V_s increased as hydration reaction of cement evolved. V_s tends to be stable (slope < 1) after 6-15 hours of hydration reaction for the samples; 2) V_s was approximately 1700-2100 m/s for hardened (> 20 hrs) mortar; 3) At any time node, V_s was on the order of 0.37 > 0.43 > 0.50 of w/c without any chemical admixtures. 4) Retarder significantly influenced the hydration reaction of

cement (approximately 3 h and 5 h with dosages of 195 mL/100kg and 220 mL/100kg, respectfully). 5) With the use of accelerator, V_s increased before 9 h and decreased after 9 h, which means accelerator will decrease the shear modulus of hardened mortar. Figure 5.8 illustrates literature comparison of shear wave velocity of mortar mixtures without chemical admixtures. V_s obtained from P-RAT system (Soliman et al. 2015) and BE system (Liu et al. 2014) were generally higher than V_s from BE system, but both shown a similar increasing rate with time. This study provides a wider range of elapsed time (0-24 hrs) of V_s than Soliman et al. 2015, Liu et al. 2014, Zhu et al. 2011, and Carette and Staquet 2015.
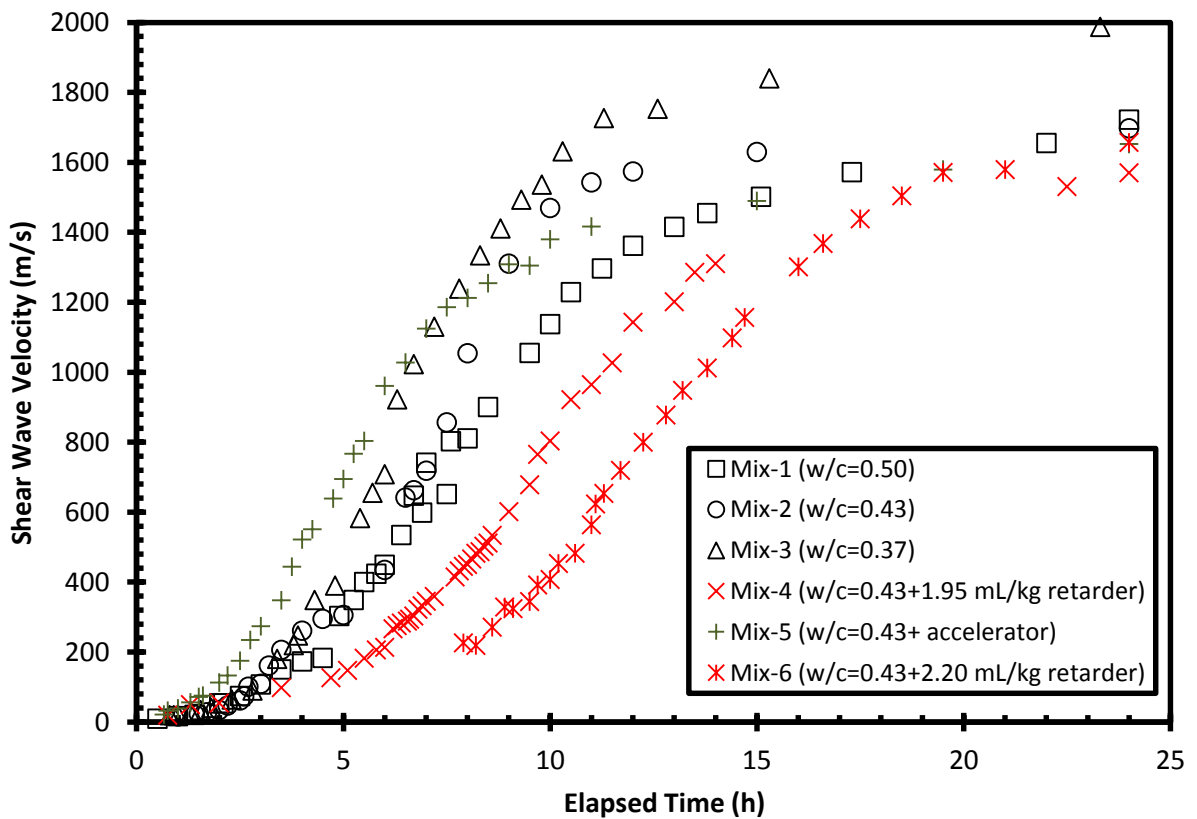

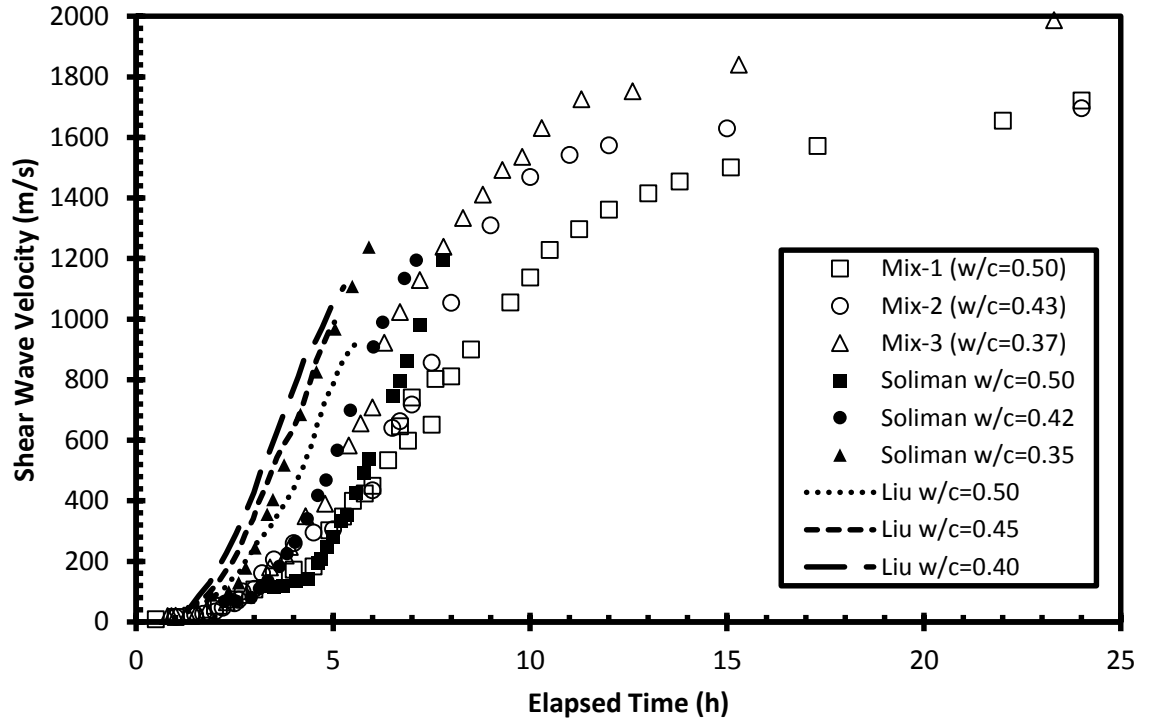Figure 5.7. Shear Wave Velocity versus Elapsed Time

Figure 5.8. Comparison of Shear Wave Velocity Results

5.4. DETERMINATION OF SET TIMES WITH SHEAR WAVE VELOCITY METHOD

Initial and final setting times can be determined from V_s curve (Soliman et al.

2015). However, due to the discretization of the measured data points, a curve fitting

method is needed to achieve smooth and equational V_s curves. Weibull distribution

(Weibull 1951) (Equation 4), Log-normal distribution (Ahrens 1954) (Equation 5), and

Gamma distribution (Moschopoulos 1984) (Equation 7) were used to fit the V_s curve of

six mortar mixtures. Key parameters, such as alpha and beta in Weibull distribution, were

calculated with the minimum variance between cumulative distribution function and

measured V_s. To quantify how well a data fit these three statistical models, the coefficient

of determination (R^2) was used. All fitting methods shown very good suitability (R^2

ranged from 0.992 to 0.999) (Table 5.2). In this study, Log-normal cumulative

distribution (Equation 5) was selected to represent V_s curves, and Log-normal probability

distribution (Equation 6) was selected to describe the slope of V_s curves.

Because the above fitting methods only have two controlled parameters and

without description of inflection point, equation for the soil-water characteristic curve

(SWCC) (Fredlund and Xing 1994) (Equation 8) was introduced to fit the V_s curve.

The comparison of the four fitting methods was plotted in Figure 5.9 and all

fitting curves were plotted in Figure 5.10.

$$y = 1 - e^{-\left(\frac{x}{\beta}\right)^{\alpha}} \tag{4}$$

$$y = \frac{1}{2} + \frac{1}{2}\text{erf}(\frac{\ln x - \mu}{\sqrt{2}\sigma}) \tag{5}$$

$$y = \frac{1}{x\sigma\sqrt{2\pi}} e^{-\frac{(\ln x - \mu)^2}{2\sigma^2}} \tag{6}$$

$$y = \frac{1}{\Gamma(\alpha)}\gamma(\alpha, \beta x) \tag{7}$$

$$\theta = \theta_s [\frac{1}{\ln(e + (\psi/a)^n)}]^m \tag{8}$$

$$f(\psi) = \frac{mn(\psi/a)^{n-1}}{a[e + (\psi/a)^n]\{\log[e + (\psi/a)^n]\}^{m+1}} \tag{9}$$

It was observed that there was a peak in each slope (Figure 5.11 and 5.12), which

indicates the fastest increasing rate of shear wave velocity (maximum derivative) and

probably the strongest chemical reaction. It is obvious that the final setting time and t-

peak of the slope (derivative curve) are very closed. With the linear equation

y=0.96x+0.17 and R^2 of 0.979, it is reasonable to conclude that the time corresponded to

the largest slope (i.e. maximum V_s increasing rate) of V_s curve is final setting time
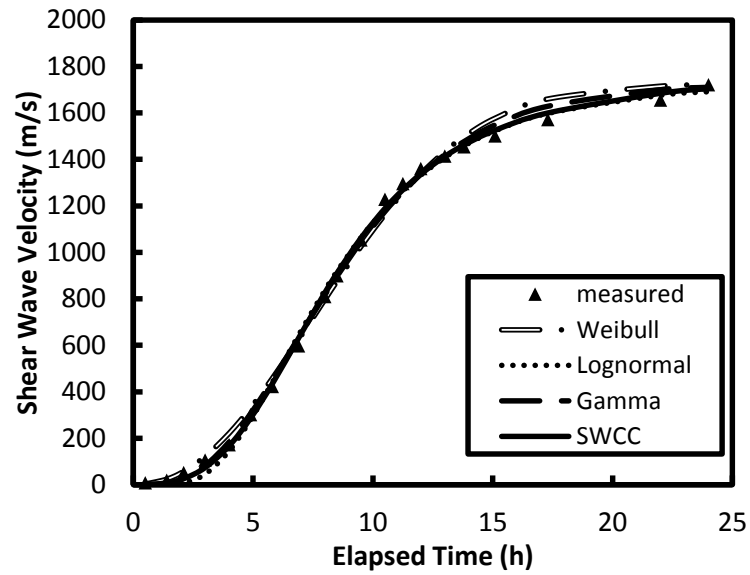
(Figure 5.13).

Figure 5.9. Fitting Curves of Weibull, Log-normal, Gamma, and SWCC Methods
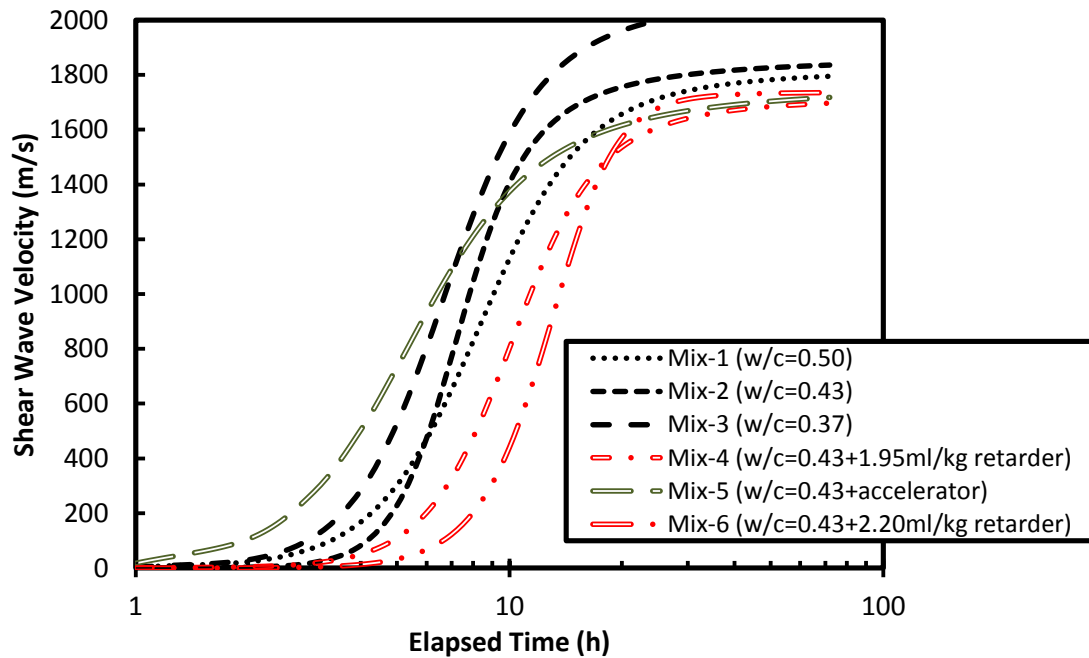

Figure 5.10. Fitted Curves (SWCC Method) of Shear Wave Velocity versus Time
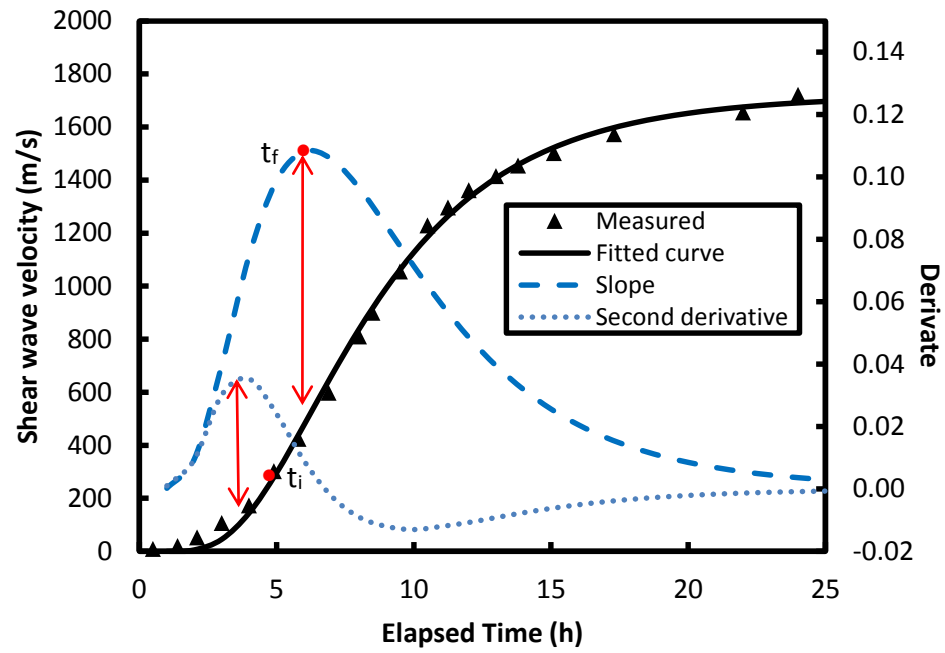
Figure 5.11. Slope and Second Derivative of V_s Curves
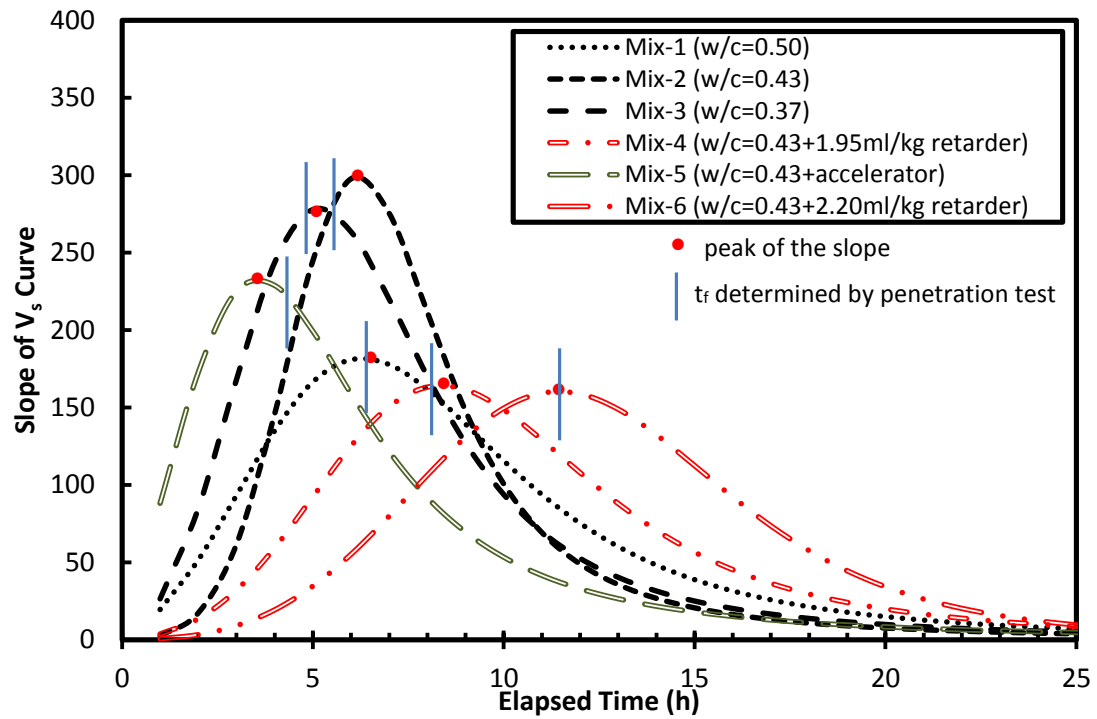

Figure 5.12. Slope of V_s versus Time
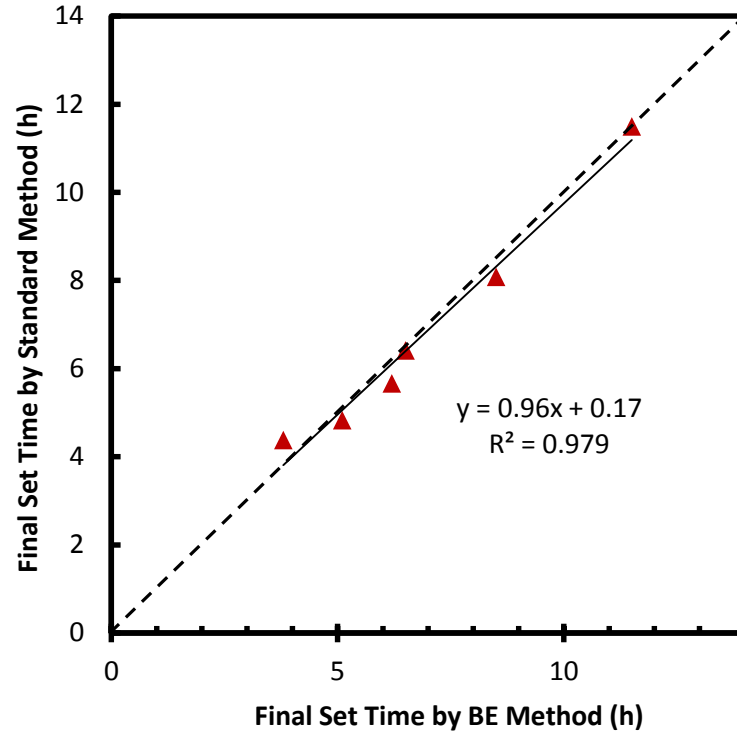
Figure 5.13. Comparison of Final Set Time between Standard Method and BE Method

There are two methods to determine initial setting time with shear wave velocity method proposed in this study. One is using parameter a in SWCC equation (Fredlund and Xing 1994), which has a linear relationship with initial setting time, i.e. t_i=0.70a-0.50 (Figure 5.14). The other is using the time of maximum second derivative curve, i.e. t_i=1.04x+1.05, where x is the time (h) corresponding to the peak of second derivative V_s curve (Figure 5.15). Both methods were reliable (R^2 of 0.981 and 0.950 respectively).

Carette and Staquet (2015) proposed that the initial setting time corresponds to the peak of the shear wave velocity derivative; the final setting time corresponds to the peak of the Young's modulus derivative. However, the peak of the shear wave velocity derivative corresponds to final setting time in this study.

Figure 5.14. Determination of Initial Set Time with SWCC Method

Figure 5.15. Determination of Initial Set Time with V_s'' Method
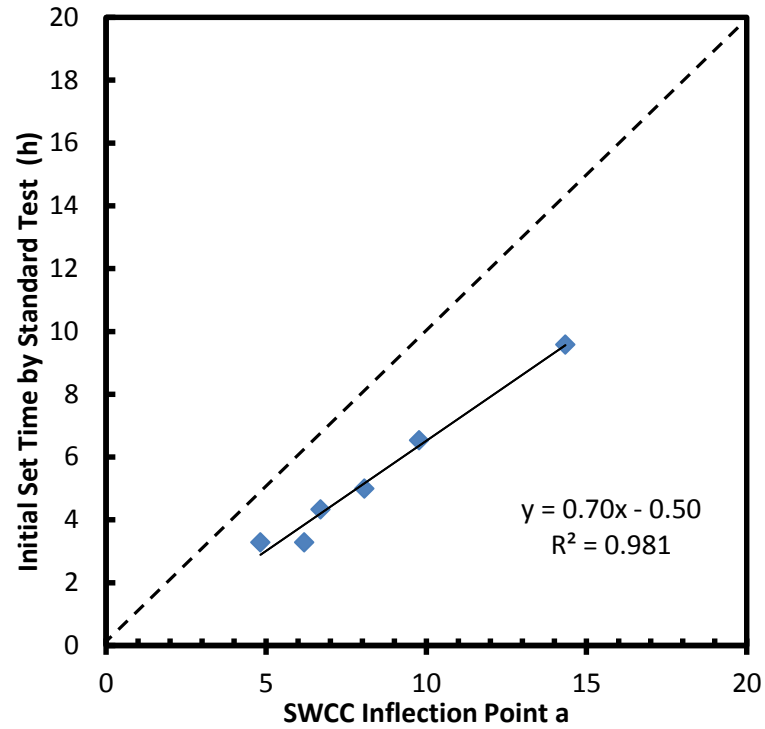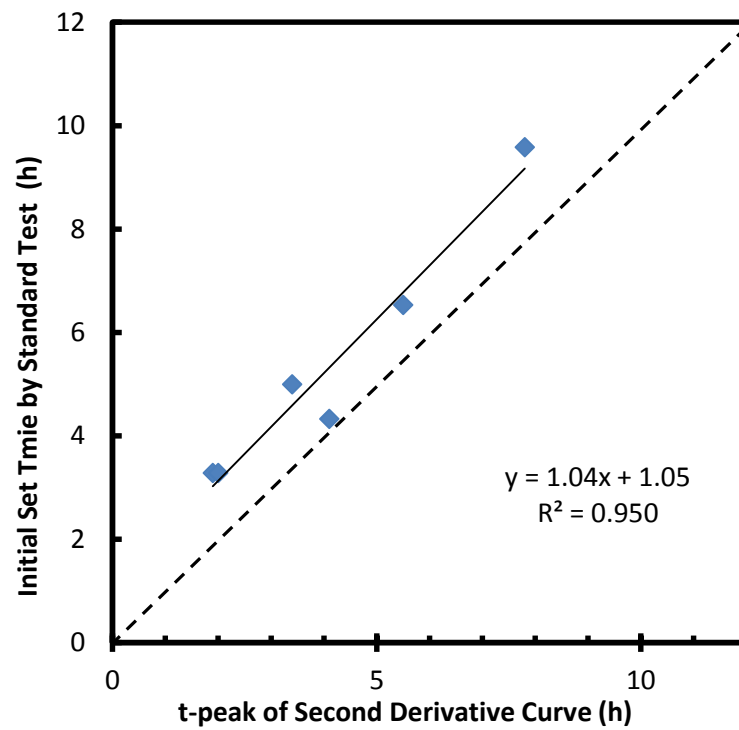
Table 5.2. Parameters of Weibull, Log-normal, Gamma Distributions, and SWCC Fitting

Fitting methods	Parameters	Mix-1	Mix-2	Mix-3	Mix-4	Mix-5	Mix-6
Weibull	α	2.178	2.651	2.303	3.018	1.773	3.384
	β	9.953	8.933	8.124	11.286	6.955	14.083
	R^2	0.996	0.995	0.994	0.998	0.992	0.999
Lognormal	μ	2.097	2.031	1.904	2.285	1.695	2.511
	σ	0.516	0.416	0.486	0.411	0.637	0.331
	R^2	0.998	0.996	0.998	0.994	0.997	0.996
Gamma	α	3.934	5.795	4.422	6.447	2.707	9.227
	β	2.295	1.405	1.665	1.617	2.341	1.396
	R^2	0.998	0.996	0.997	0.996	0.995	0.998
SWCC (Fredlund and Xing 1994)	a	8.068	6.696	6.190	9.778	4.817	14.346
	n	3.015	5.019	3.464	3.683	2.677	4.047
	m	2.266	1.656	1.921	2.162	1.825	3.707
	R^2	0.999	0.995	0.999	0.997	0.998	0.999

5.5. EVOLUTION OF PULSE WAVE VELOCITY

The evolution of pulse wave velocity (V_p) with elapsed time was plotted in Figure 5.16. The V_p increased dramatically during the setting process of mortar mixtures. At the same elapsed time, mortar with low w/c has higher V_p than those with high w/c, when there is no chemical admixtures. It was also observed that the using of accelerator lowered down V_p after 8 h of hydration time. There was no reading from the UPV device in the initial state (t < 4 h) of mortar. V_p can be affected by air voids in fresh cementitious materials (Zhu et al. 2011). Compared to the V_p measured by Liu et al. 2014, V_p in this study was slightly low.

5.6. DETERMINATION OF SET TIMES WITH CALORIMETRY METHOD

The rate of heat evolution with mortar mixtures was achieved by calorimetry tests, as shown in Figure 5.17. The process of cement hydration can be broken down into five
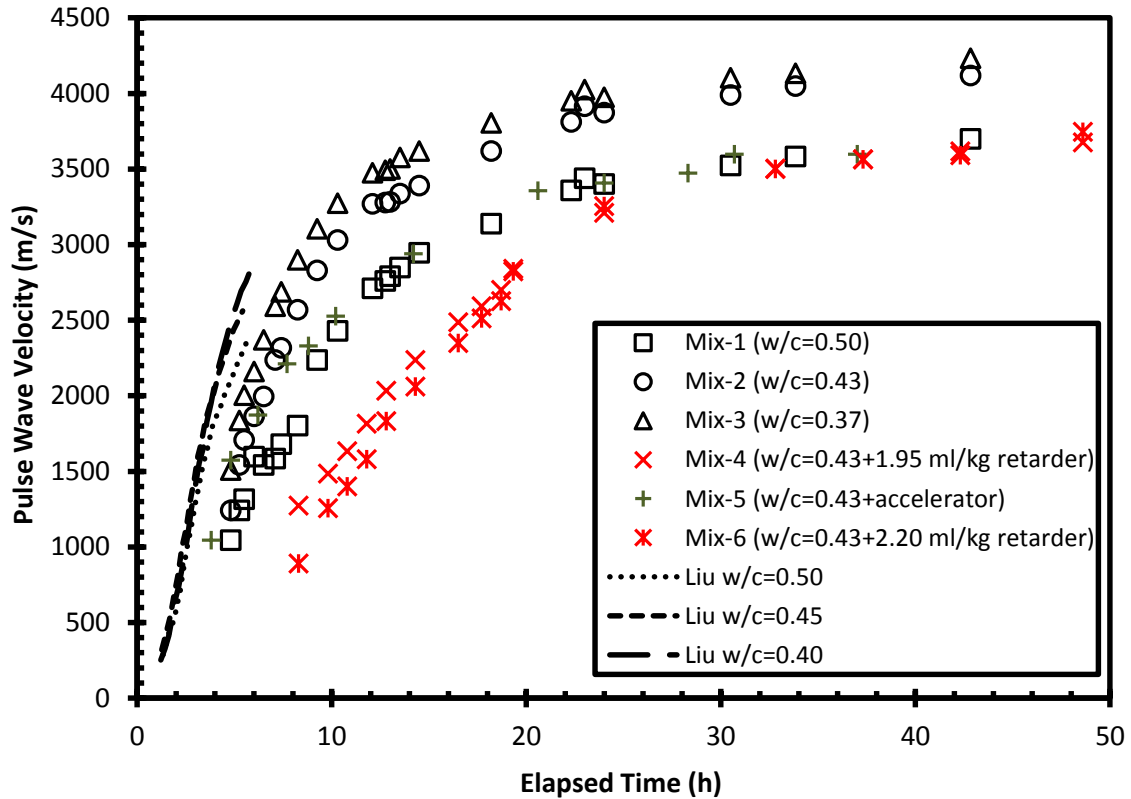
Figure 5.16. Pulse Wave Velocity versus Elapsed Time

stages. The first stage generated a large amount of heat rapidly when cement particles were exposed to water. Hydration activity reduced to a slow rate during Stage 2, which is also named as dormant period. Mortar with retarder (Mix-4 and 6) had a long dormant period. Stage 3 (acceleration) represents the heat of formation of ettringite, a quick crystallization followed by a rapid reaction of CH and CSH was formed (Soliman et al. 2015); both initial set (beginning of solidification) and final set (complete solidification and beginning of hardening) were achieved in this period. There were still hydration products formed during Stage 4 (Deceleration) and Stage 5 (Diffusion Limited), however, the hydration rate decreased to a very low level. (Garboczi et al. 2014)

Figure 5.18 illustrates the method for determining set times from calorimetry test result of mortar mixture 1 (Ge et al. 2009). First derivative of the rate of heat evolution with time is plotted is this method. Initial set time correlates to time of the highest value of the first derivate curve, at which the increasing rate of heat generation is the fastest (inflection point of heat evolution). Final set time correlates to the time when the first derivative of heat evolution curve decrease to zero, which indicates the rate of heat generation starts to slow down (maximum heat generation point). Figure 5.19 shows a correlation between initial set time determined by standard test and the time at inflection point of heat evolution. Initial set time determined by calorimetry method was achieved by applying the linear equation. The determination of final set time with maximum heat generation was plotted in Figure 5.20. Sandberg and Liberman (2007) proposed two methods to predict set times. Derivatives method defines the initial set as the time of maximum second derivative, and the final set as the time of the maximum first derivative. Fractions method defines the initial and final set as the time when the measured temperature is in a certain percentage between the baseline and the maximum temperature.

Table 5.3 is the summary of set times with different determination methods. For initial set time, bender element method with parameter a in SWCC equation has higher R-squared than BE method with second derivative of Vs, and both are more reliable than calorimetry method (R^2 of 0.910). But it is important to note that the second derivative of Vs is more common to be used, regardless the fitting methods. Using BE method (R^2=0.979) to determine the final set time is also better than calorimetry method (R^2=0.908).
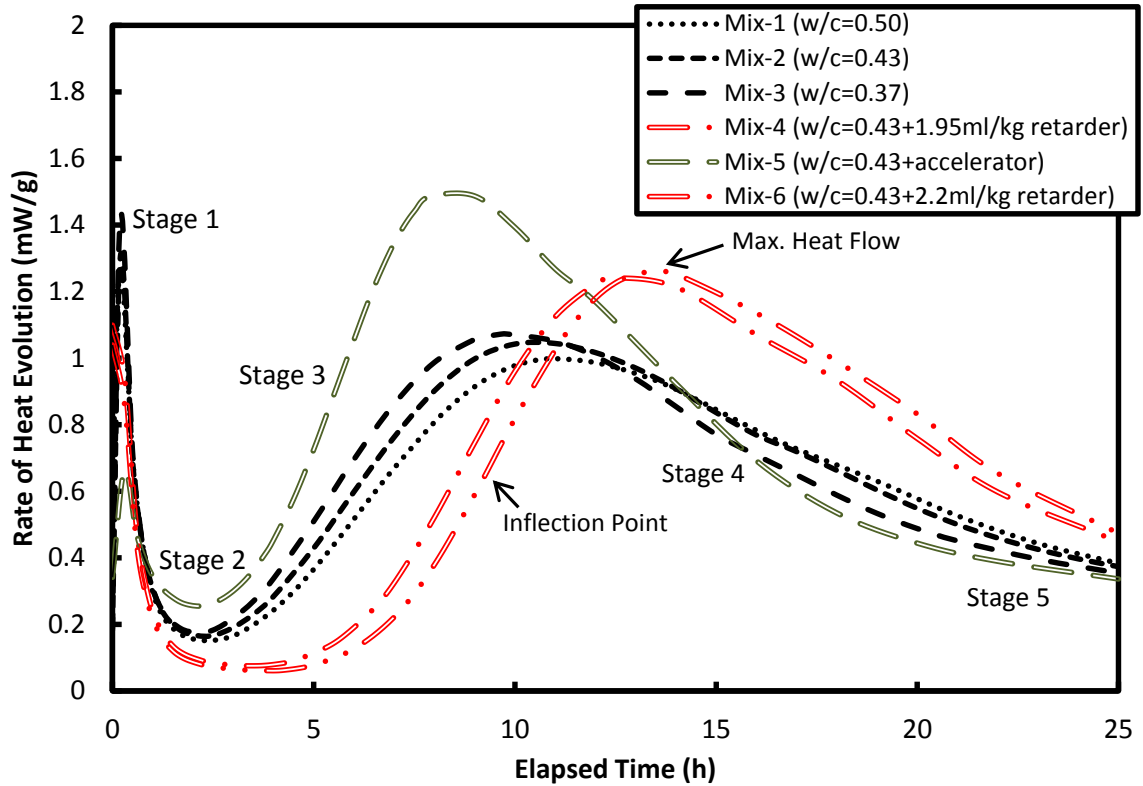
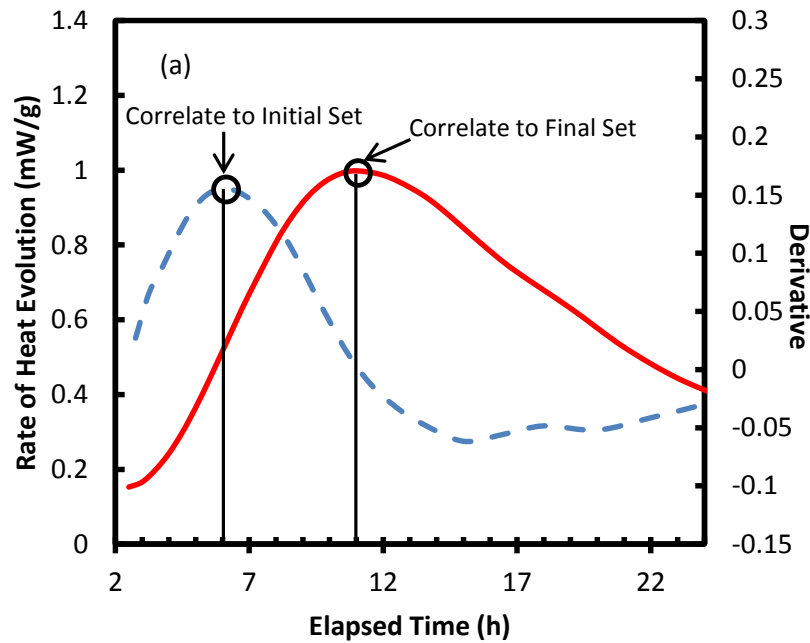Figure 5.17. Evolution of Heat of Hydration with Time

Figure 5.18. First Derivative of Heat of Hydration with Time (a) Derivate of Mix-1 (b)
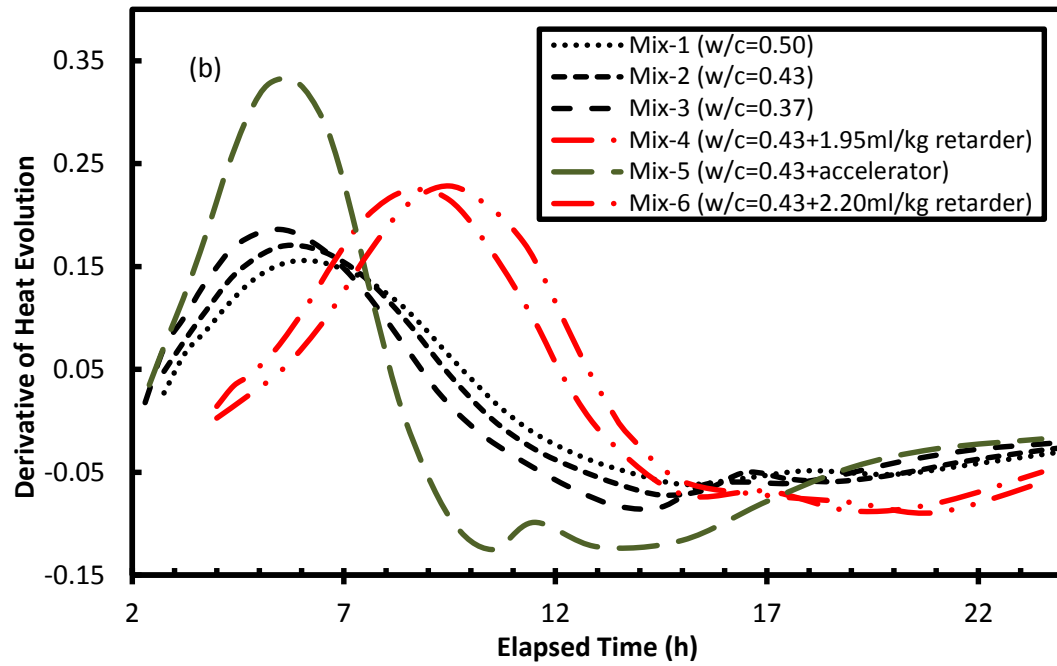Derivative of Six Mixtures

Figure 5.18. First Derivative of Heat of Hydration with Time (a) Derivate of Mix-1 (b) Derivative of Six Mixtures (cont.)
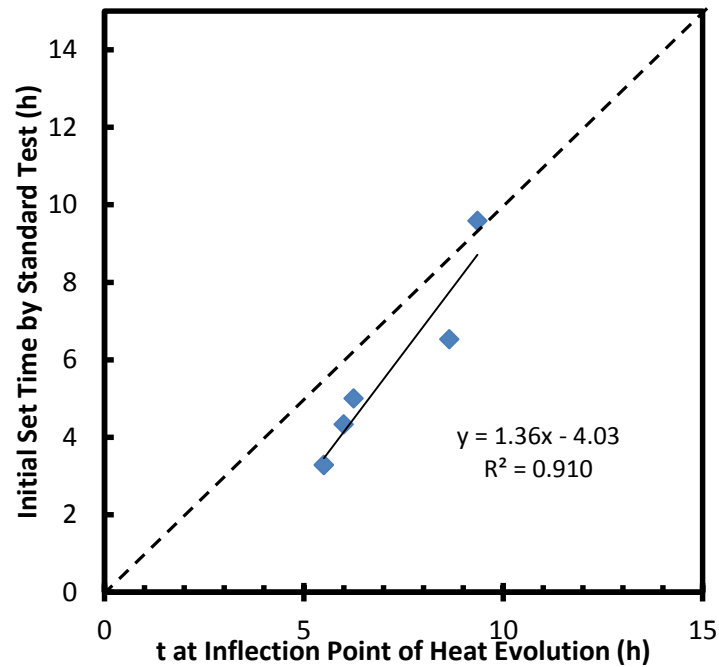

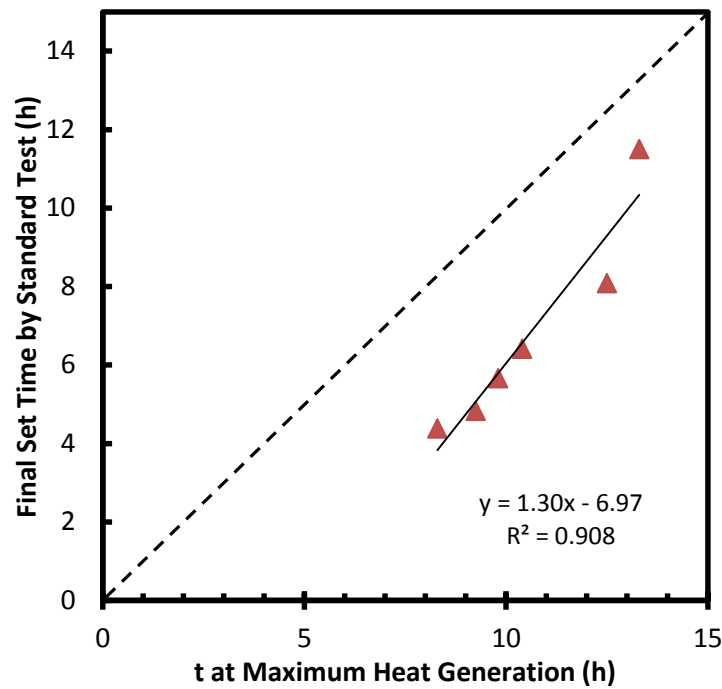Figure 5.19. Determination of Initial Set Time with Calorimetry Method

Figure 5.20. Determination of Final Set Time with Calorimetry Method

Table 5.3. Determination of Set Times with Different Methods

Mortar	Initial Set (h)				Final Set (h)		
	Standard	BE (V_s'')	BE (a)	Calorimetry	Standard	BE	Calorimetry
Mix-1	5.00	4.59	5.16	4.48	6.42	6.50	6.56
Mix-2	4.33	5.32	4.20	4.14	5.67	6.20	5.78
Mix-3	3.28	3.03	3.85	3.46	4.83	5.10	5.07
Mix-4	6.53	6.78	6.36	7.75	8.08	8.50	9.30
Mix-5	3.28	3.13	2.88	3.46	4.38	3.80	3.83
Mix-6	9.58	9.17	9.56	8.71	11.50	11.50	10.34
R^2	-	0.950	0.981	0.910	-	0.979	0.908

5.7. DYNAMIC PROPERTIES

Both V_p and V_s have a similar increasing rate (Figure 5.21). V_s/V_p ratio increased

rapidly (from less than 0.20 to 0.58) during the first 10 h of setting process; however,

V_s/V_p decreased slightly between 10 h and 20h, and remained at a relatively constant

value (0.50) after 20 h, as shown in Figure 5.22. Although w/c has a great influence on V_s and V_p, it did not affect the value of V_s/V_p.

Poisson's ratio was calculated based on V_s/V_p ratio (Equation 8). It was initially high and decreased to 0.32-0.36 after 20 h of hydration reaction (Figure 5.23). Swamy (1971) found that Poisson's ratio of 1 day aged mortar is 0.27, of hardened mortar is 0.21, which agree with that Poisson's ratio is generally higher in cementitious materials at early age. In addition, there was no consistent relationship between Poisson's ratio and water cement ratio or curing age (Mehta and Monteiro 2006).

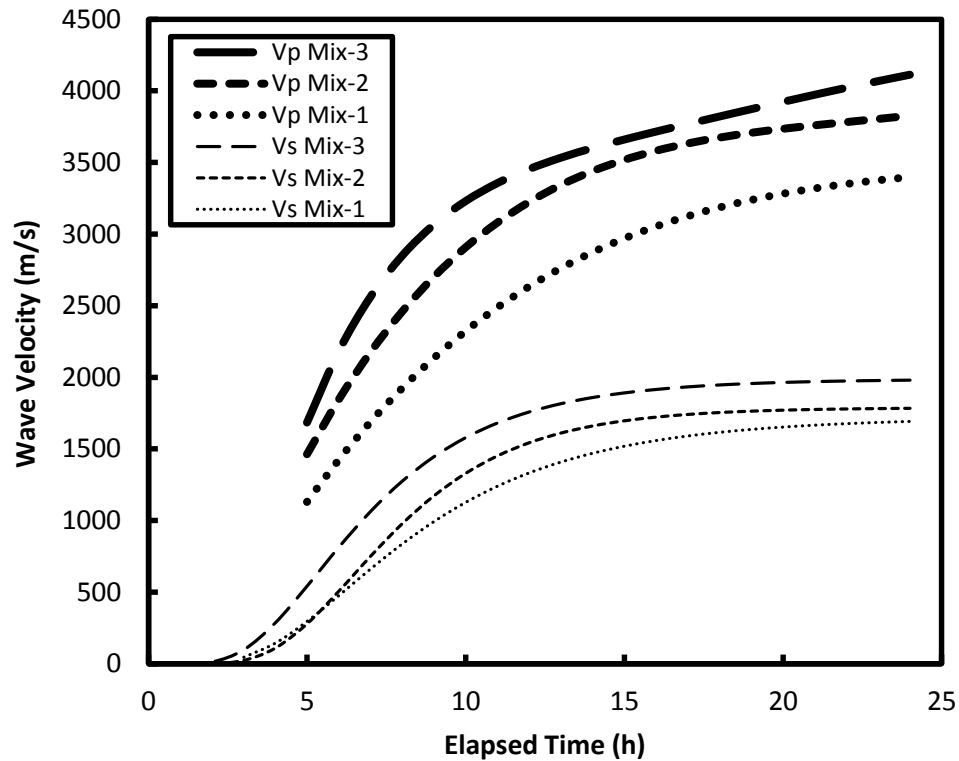$$\mu = \frac{1 - 2(\frac{V_s}{V_p})^2}{2 - 2(\frac{V_s}{V_p})^2} \tag{8}$$

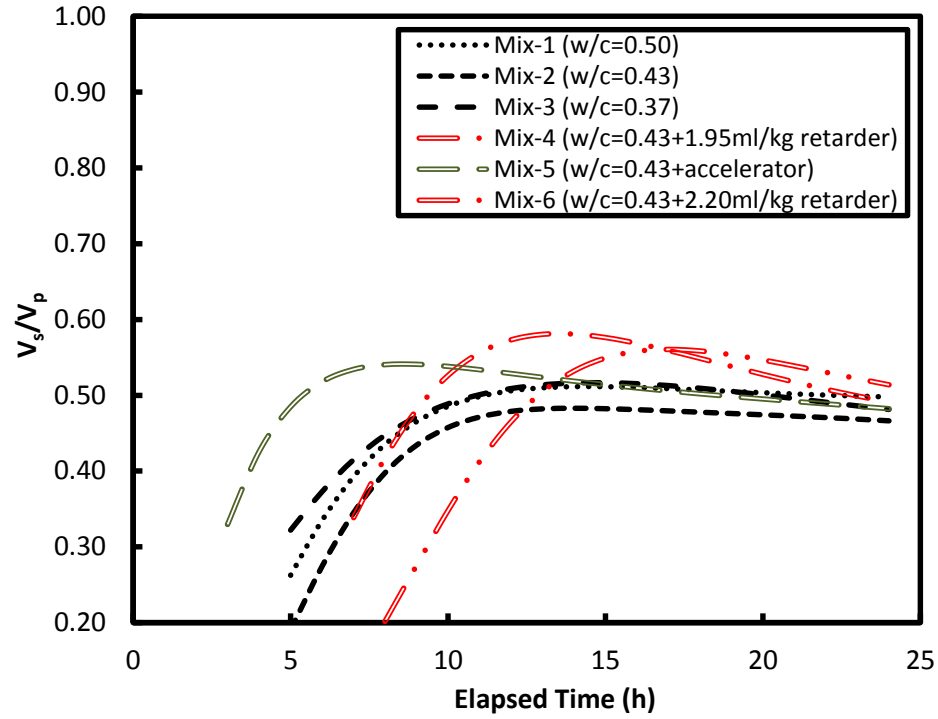Figure 5.21. Evolution of Shear and Pulse Wave Velocities with Time
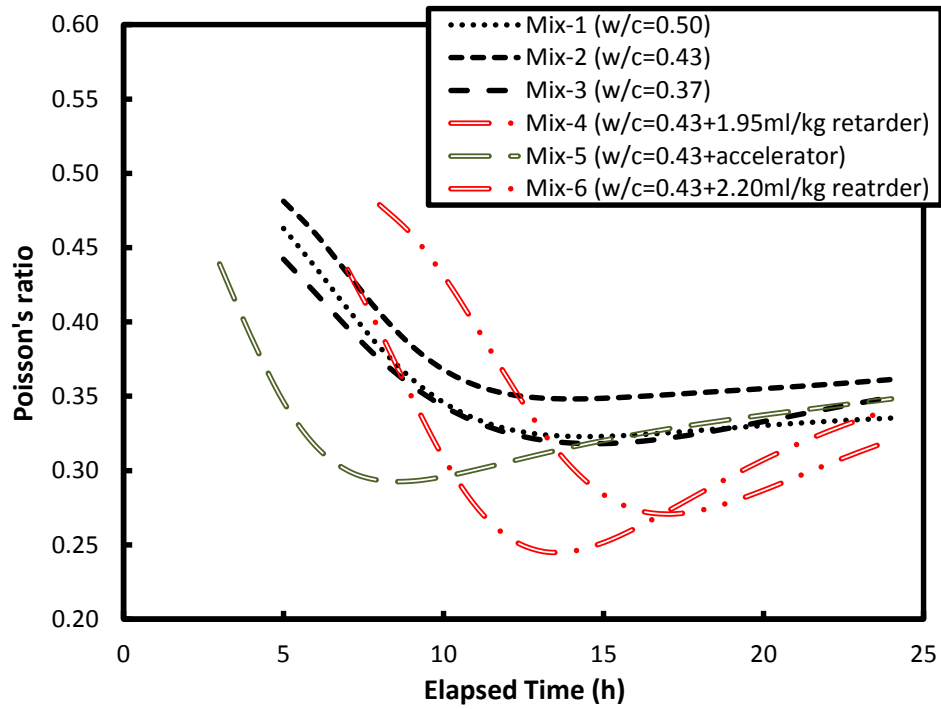
Figure 5.22. Evolution of V_s/V_p with Time

Figure 5.23. Evolution of Poisson's Ratio with Time

Dynamic moduli (shear modulus G, Young's modulus E, and bulk modulus K) were calculated according to V_s, V_p, and the density r of mortar mixtures, as follows:

$$G = \rho V_s{}^2 \tag{9}$$

$$E = 2\rho V_s{}^2(1 + \mu) \tag{10}$$

$$K = \rho V_p{}^2 - \frac{4}{3}G \tag{11}$$

The evolutions of shear modulus, Young's modulus, and bulk modulus with time for mortar mixtures were plotted in Figure 5.24, Figure 5.25, and Figure 5.26, respectively. At the same elapsed time of mortar without admixtures, the dynamic moduli (G, E, and K) of was on the order of $0.37 > 0.43 > 0.50$ of w/c. Similar increment rate of dynamic moduli were recorded with respect to elapsed time in three mortar mixtures during hydration. The increase of dynamic modulus during hydration was attributed to the decay of Poison's ratio (Figure 5.27).

Obtaining dynamic properties of mortar at early age with V_s, V_p and r has advantages: (1) Continuous monitoring. Shear modulus could be obtained immediately after casting, while Yong's and bulk modulus could be obtained after 5 hrs of casting. (2) Because of its non-destructive nature, this application can be used in the field and avoid test of different samples.
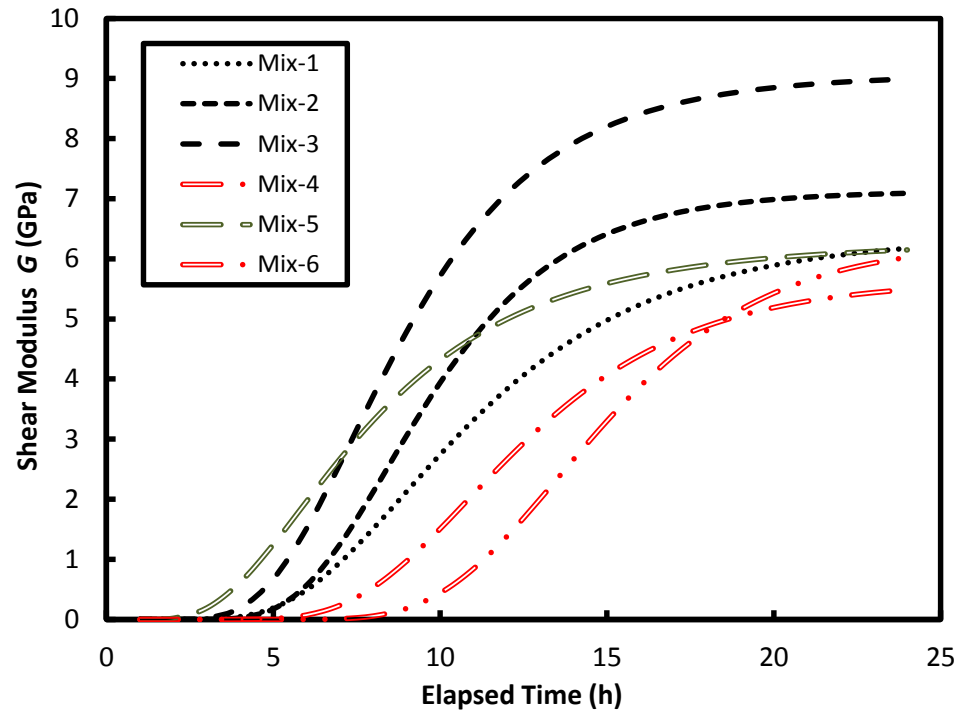
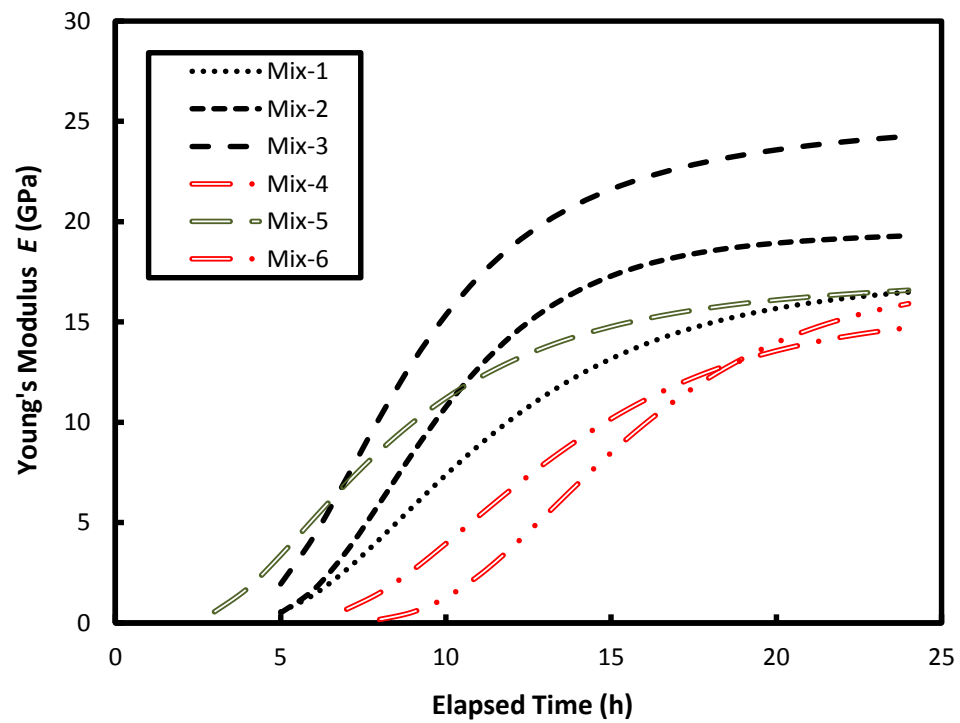Figure 5.24. Evolution of Shear Modulus with Time

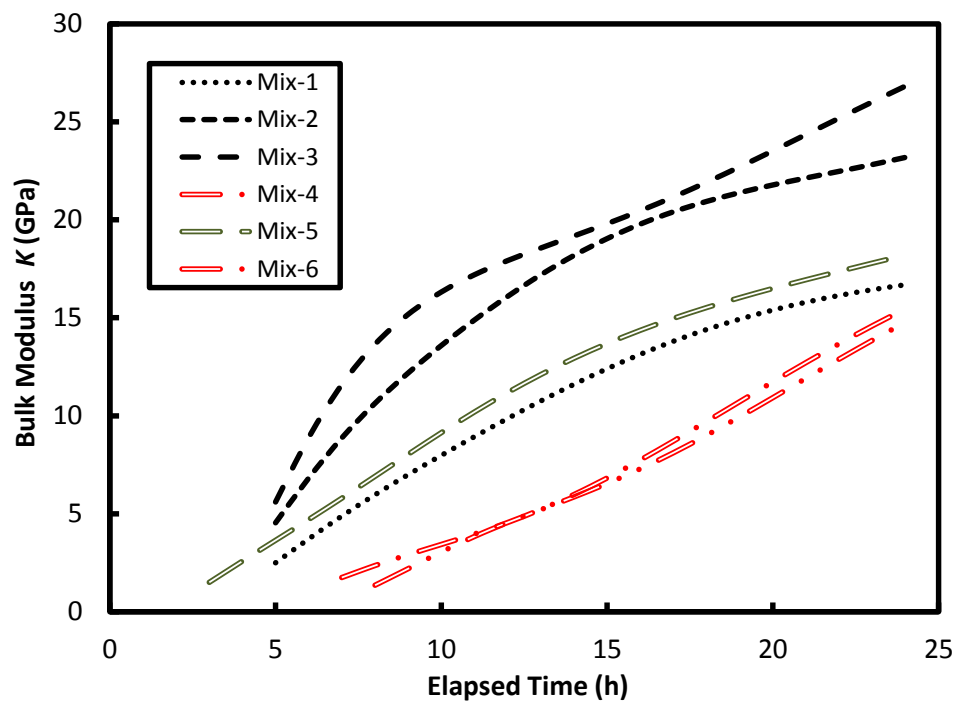Figure 5.25. Evolution of Young's Modulus with Time

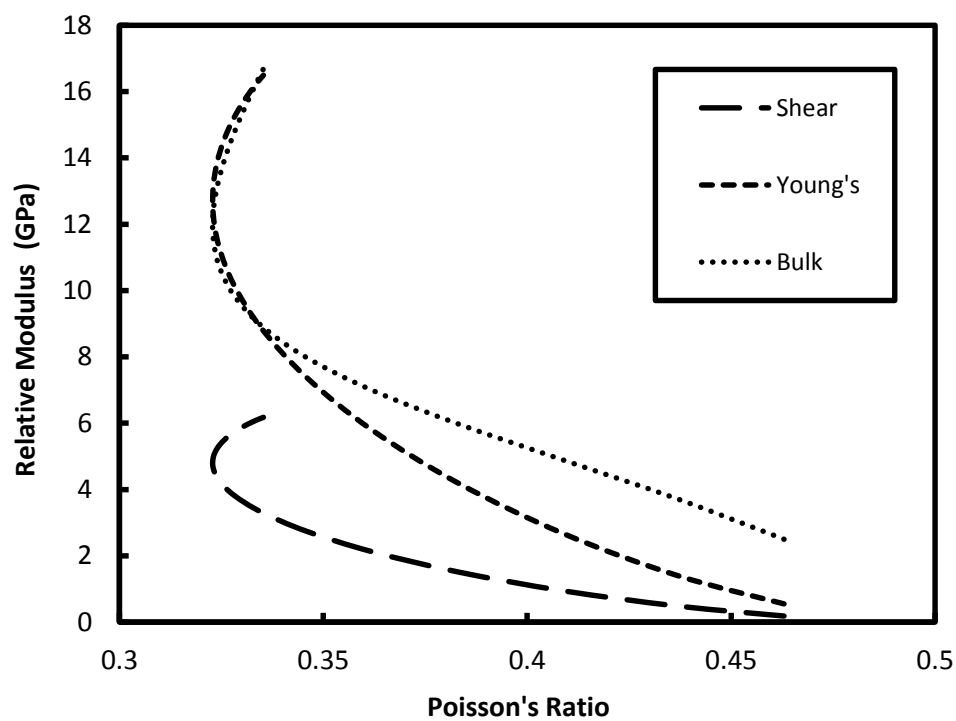Figure 5.26. Evolution of Bulk Modulus with Time

Figure 5.27. Relative Modulus versus Poisson's Ratio (Mix-1)

6. CONCLUSION AND FUTURE WORK

6.1. CONCLUSION

This study provides a guideline regarding the fabrication of BE that can be used in aggressive cement environment successfully. In summary, the following modifications were made to obtain a good bender element for aggressive cement environment: 1) increasing the size of bender element in order to obtain larger excitation energy; 2) applying a uniform primer and PVC cement instead of epoxy coating to have good flexibility, integrity and chemical resistance; 3) eliminating the silver conductivity coating to reduce the risk of electrical short-circuits; and 4) applying multi-layers of polyurethane coating to piezoceramics plates to achieve better waterproofness.

Energy approach method was proposed to determine the first arrival time of S-wave, which has benefits of convenience and less variability. Multi scale of shear wave figures have to be used in order to read first arrival times clearly. Excitation frequency did not affect the first arrival time; however, readings were not possible when excitation frequency was too small or too large.

Log-normal distribution and SWCC method were used to determine the set times. It was found that the time corresponded to the largest slope of V_s curve is final setting time, while initial setting time has a strong linear relationship with both parameter a in SWCC equation and t-peak of second derivative curve. With R^2 of 0.950 or larger, these test results were similar to those in ASTM standard test.

With the non-destructive nature and reliable results, bender element method of obtaining V_s and determining set times is a potential application in cement industry.

6.2. FUTURE WORK

More experimental data are needed to support the new proposed methods of determining setting times. Bender element technique can also be applied in cement past, normal concrete, self-consolidating concrete. The numerical simulation of mortar at early age can help with the interpretation of V_s evolution. In addition, the application of bender element method in the field projects is desired, which may require additional modifications.

BIBLIOGRAPHY

Ahrens, L. H. (1954), "The lognormal distribution of the elements (a fundamental law of geochemistry and its subsidiary)," Geochimica et Cosmochimica Acta, 5, 49-73.

Amziane, S. (2006), "Setting time determination of cementitious materials based on measurements of the hydraulic pressure variations," Cement and Concrete Research, v 36, n 2, p 295-304.

Arulnathan, R., Boulanger, R. W., and Riemer, M. F. (1998), "Analysis of bender element tests," Geotechnical Testing Journal, v 21, n 2, p 120-131.

Bate, B., Choo, H., and Burns, S. E. (2013), "Dynamic properties of fine-grained soils engineered with a controlled organic phase," Soil Dynamics and Earthquake Engineering, v 53, p 176-186.

Birgul, R. (2009), "Hilbert transformation of waveforms to determine shear wave velocity in concrete," Cement and Concrete Research, v 39, n 8, p 696-700.

Chung, C., Suraneni, P., Popovics, J. S., and Struble, L. J. (2012), "Setting time measurement using ultrasonic wave reflection," ACI Materials Journal, v 109, n 1, p 109-117.

Dyvik, R., and Madshus, C. (1985), "Lab measurements of Gmax using bender elements," Proc., Advances in the Art of Testing Soils Under Cyclic Conditions. Proceedings of a session held in conjunction with the ASCE Convention, p 186-196.

Fredlund, D.G., and Xing, A. (1994), "Equations for the soil-water characteristic curve," Canadian geotechnical journal, v 31, n 4, p 521-532.

Garboczi, E. J., Stutzman, P. E., Wang, S., Martys, N. S., Hassan, A. M., Duthinh, D., Provenzano, V., Chou, S. G., Plusquellic, D. F., Surek, J. T., Kim, S., McMichael, R. D., Stiles, M.D. (2014), "Corrosion detection in steel-reinforced concrete using a spectroscopic technique," AIP Conference Proceedings, v 1581, n 33, p 1178-1183.

Garnier, V. (1995), "Setting time study of roller compacted concrete by spectral analysis of transmitted ultrasonic signals," NDT & E International, v 28, n 1, p 15-22.

Ge, Z., Wang, K., Sandberg, P. J., and Ruiz, J. M. (2009), "Characterization and performance prediction of cement-based materials using a simple isothermal calorimeter," Journal of Advanced Concrete Technology, v 7, n 3, p 355-366.

Hofmann, M. P., Nazhat, S. N., Gbureck, U., and Barralet, J. E. (2006), "Real-time monitoring of the setting reaction of brushite-forming cement using isothermal differential scanning calorimetry," Journal of Biomedical Materials Research - Part B Applied Biomaterials, v 79, n 2, p 360-364.

Jovicic, V., Coop, M. R., and Simic, M. (1996), "Objective criteria for determining Gmax from bender element tests," Geotechnique, v 46, n 2, p 357-362.

Kang, X., Kang, G. -C., and Bate, B. (2014), "Measurement of stiffness anisotropy in kaolinite using bender element tests in a floating wall consolidometer," Geotechnical Testing Journal, v 37, n 5.

Kjellsen, K. O., and Detwiler, R. J. (1992), "Reaction kinetics of portland cement mortars hydrated at different temperatures," Cement and Concrete Research, v 22, n 1, p 112-120.

Landis, E.N., and Shah, S. P. (1995), "Frequency-dependent stress wave attenuation in cementbased materials," Journal of Engineering Mechanics, v 121, n 6, p 737-742.

Lee, J. –S., and Santamarina, J. C. (2005), "Bender elements: Performance and signal interpretation," Journal of Geotechnical and Geoenvironmental Engineering, v 131, n 9, p 1063-1070.

Leong, E. C., Yeo, S. H., and Rahardjo, H. (2005), "Measuring shear wave velocity using bender elements," Geotechnical Testing Journal, v 28, n 5, p 488-498.

Li, Z., Xiao, L., and Wei, X. (2007), "Determination of concrete setting time using electrical resistivity measurement," Journal of Materials in Civil Engineering, v 19, n 5, p 423-427.

Liang, M.T., and Wu, J. (2002), "Theoretical elucidation on the empirical formulae for the ultrasonaic testing method for concrete structures," Cement and Concrete Research, v 32, n 1, p 1763-1769.

Liu, S., Zhu, J., Seraj, S., Cano, R., and Juenger, M. (2014), "Monitoring setting and hardening process of mortar and concrete using ultrasonic shear waves," Construction and Building Materials, v 72, p 248-255.

Ma, H. (2013), "Multi-scale Modeling of the Microstructure and Transport Properties of Contemporary Concrete," PhD, The Hong Kong University of Science and Technology, Hong Kong.

Marjanovic, J., and Germaine, J. T. (2013), "Experimental study investigating the effects of setup conditions on bender element velocity results," Geotechnical Testing Journal, v 36, n 2.

Mehta, P. K., and Monteiro, P. J. M. (2006), "Concrete: Microstructure, Properties, and Materials," McGraw-Hill.

Montoya, B. M., Gerhard, R., DeJong, J. T., Wilson, D. W., Weil, M. H., Martinez, B. C., and Pederson, L. (2012), "Fabrication, operation, and health monitoring of bender elements for aggressive environments," Geotechnical Testing Journal, v 35, n 5.

Moschopoulos, P. G. (1984), "The distribution of the sum of independent gamma random variables," Annals of the Institude of Statistical Mathematics, v 37, p 541-544.

Rahhal, V., and Talero, R. (2009), "Calorimetry of Portland cement with silica fume, diatomite and quartz additions," Construction and Building Materials, v 23, n 11, p 3367-3374.

Sayers, C. M. and Dahlin, A. (1993), "Propagation of ultrasound through hydrating cement pastes at early times," Advanced Cement Based Materials, v 1, n 1, p 12-21.

Sandberg, J. P. and Liberman, S. (2007), "Monitoring and evaluation of cement hydration by semi-adiabatic field calorimetry," Concrete Heat Development: Monitoring, Prediction, and Management, NY: Curran Associates. Inc., v 241, p 13-24.

Soliman, N. A., Khayat, K. H., Karray, M., and Omran, A. F. (2015), "Piezoelectric ring actuator technique to monitor early-age properties of cement-based materials," Cement and Concrete Composites.

Swamy, R. N. (1971), "Dynamic Poisson's ratio of portland cement paste, mortar and concrete," Cement and Concrete Research, v 1, n 5, p 559-583

Trtnik, G., Turk, G., Kavcic, F., and Bosiljkov, V. B. (2008), "Possibilities of using the ultrasonic wave transmission method to estimate initial setting time of cement paste," Cement and Concrete Research, v 38, n 11, p 1336-1342.

Viggiani, G., Atkinson, J. H. (1995), "Interpretation of bender element tests," Geotechnique, v 45, p 149-154.

Weibull, W. (1951), "A statistical distribution function of wide applicability," Journal of Applied Mechanics-Transactions, v 18, n 3, p 293-297.

Yaman, I.O., Inci, G., Yesiller, N., Aktan, H. M. (2001), "Ultrasonic pulse velocity in concrete using direct and indirect transmission," ACI Materials Journal, v 98, n 6, p 450-457.

Yamashita, S., Kawaguchi, T., Nakata, Y., Mikamt, T., Fujiwara, T., Shibuya, S. (2009), "Interpretation of international parallel test on the measurement of G max using bender elements," Soils and Foundations, v 49, n 4, p 631-650.

Zhang, G., Zhao, J., Wang, P., and Xu, L. (2015), "Effect of HEMC on the early hydration of Portland cement highlighted by isothermal calorimetry," Journal of Thermal Analysis and Calorimetry, v 119, n 3, p 1833-1843.

Zhu, J., Thai, Y. –T., and Kee, S. –H. (2011), "Monitoring early age property of cement and concrete using piezoceramic bender elements," Smart Materials and Structures, v 20, n 11.

Zhu, J., Kee, S. –H., Han, D., and Tsai Y. –T. (2011), "Effects of air voids on ultrasonic wave propagation in early age cement pastes," Cement and Concrete Research, v 41, n 8, p 872-881.

VITA

Jianfeng Zhu was born in Guangdong, China. He earned his bachelor's degree in Civil Engineering from Shenzhen University, China in June 2013. He has been a graduate student in the department of Civil, Architectural and Environmental Engineering at Missouri University of Science and Technology and worked as a graduate research assistant under Dr. Bate Bate from August 2013 to October 2015. He received his Master's degree in Geotechnical Engineering at Missouri University of Science and Technology in December 2015.